Polymer 49 (2008) 2781–2796

Contents lists available at ScienceDirect

Polymer

journal homepage: www.elsevier.com/locate/polymer

Feature Article

Progress in control of microdomain orientation in block copolymers – Efficiencies of various external fields

Shinichi Sakurai

Department of Polymer Science and Engineering, Kyoto Institute of Technology, Sakyo-ku, Kyoto 606-8585, Japan

ARTICLE INFO

Article history:
Received 25 September 2007
Received in revised form 5 March 2008
Accepted 7 March 2008
Available online 15 March 2008

Keywords:
Block copolymers
Microphase-separated structure
Orientation by external fields
Magnetic fields
Directional coalescence
Solvent evaporation-mediated fields

ABSTRACT

Recent progresses in control of orientation for block copolymer microdomains using external fields, such as force fields, electric fields, and magnetic fields will be reviewed. Since it has been more recognized that such explicit external fields are not necessarily required, implicit (unconscious) external fields, which mean those imposed automatically onto block copolymers, irrespective of intention, will also be covered under categories of "surface fields" and "directional fields", where self-organizing abilities of block copolymers are utilized for performance of spontaneous orientation (or in other words self-orientation). Although some of these phenomena of the self-orientation have been already used in application-oriented researches towards nanotechnology, the mechanisms of self-orientation still remain ambiguous. Moreover, although there have been reported interesting and significant findings on the self-orientation in the recent decades, it cannot be stated that the individual findings are well correlated with each other to draw formulated cognition. Therefore, in this feature article, we systematically discuss them under the new categories of the implicit external fields for a better understanding of phenomena and hopefully mechanisms of microdomain orientation.

1. Introduction

Block copolymers are fascinating materials in terms of both science and technology, because they exhibit beautiful structures in a few tens of nanometers due to microphase separation resulting from strong segregation between constituent block chains comprising different chemical species [1–3]. Not only the size of the microdomains is uniform, but they order regularly in space, forming macrolattice (crystal-like structures but the size of the unit cell is much larger than the crystals). Depending on the fraction (ratio of volumes) of the constituent block chains, the microdomain shape can be either spherical, cylindrical, gyroid, or lamellar, for which the relevant packing regularity is BCC (body-centered cubic), hexagonal, cubic with $Ia\bar{3}d$ space group symmetry (so-called double-gyroid), or one-dimensionally alternating, respectively. Melt phase behaviors and how to control the microdomain size and shape have been well understood in principle for A–B and A–B–A type most simple chain architectures [1–3]. The microdomain structures have been attracting interests to produce nanotemplates for lithography, as well as introducing a pathway to a promising practical application of a self-assembling ability of block copolymers in nanometer scale [4–9]. It is needless to state that the block copolymers self-assemble into multi-layers of the regularly arranged microdomains. However, a single-layered film covering on a substrate has been used as a photoresist in a soft-lithography technology [5] so that control of the microdomain orientation in thin films attracts practical interests. There is a notable application-directed study for ultrahigh density fabrication such as those in magnetic storage, through formation of magnetic nanodots by utilizing a metal-containing block copolymer, polystyrene-*block*-polyferrocenylethylmethylsilane, forming perpendicularly-oriented cylinders in a thin film [10]. For those kinds of applications, controlling microdomain orientations in thin films is one of the most important key issues in recent years. It is needless to state that controlling microdomain orientations in thicker films is also important, especially for the study of understanding precise structure–mechanical property relationship [11–13], since physical properties of block copolymers strongly depend on the morphology. Not only the morphology, but the orientations of microdomains are also the key factors to be taken into account in order to control materials properties more efficiently, such as imparting anisotropy of properties. To control orientation of microdomains is therefore one of the fundamental ways to novel specialty materials. Mechanical alignment is an effective way [14] and there are varieties of mechanical force fields to apply. Since there is an excellent review thoroughly covering varieties of the force fields [11], in the current article, some of recent progress in control of microdomain orientation will be featured, especially external fields other than the force fields. Furthermore, I introduce here a new category of

E-mail address: shin@kit.jp

0032-3861/$ – see front matter © 2008 Elsevier Ltd. All rights reserved.
doi:10.1016/j.polymer.2008.03.020

external fields, based on recent outcomes of spontaneous microdomain orientations, which should be referred to as "implicit (unconscious) external fields" because no explicit external field such as mechanical force, electric or magnetic fields are applied. In other words, the fields are ascribed to new types of a self-organization ability of block copolymers resulting in spontaneous orientation.

The outline of this article is as follows; first, some recent progress using explicit external fields, such as force fields, electric fields, and magnetic fields will be reviewed. Then the unconscious (implicit) fields will be summarized. Surface-mediated phase separation and resultant directional solidification may be relevant to this category. Therefore, this can be referred to as "surface fields" and "directional fields", covering *forced surface-mediation* via neutralization of the surface free energy, or via utilizing a patterned substrate of which surface is chemically or topographically modulated. Moreover, interesting phenomena of microdomain orientation induced by solvent evaporation will be discussed, as well as imposing temperature gradients, which have also been reported recently. This is a straightforward way to induce the directional field, having been technologically applied under the name of the "zone heating".

2. Force fields

Ordering phenomena of block copolymer microdomains under shear fields have been intensively studied in connection with corresponding rheological response [15]. It has been found that block copolymer micelles exhibit similarity to other cubic crystalline systems, for instance colloidal crystals [16–20]. Imposing steady shear on block copolymer micelles creates long-range order both in BCC and face-centered (FCC) cubic micellar crystals. In the FCC crystal, {111} layers normal to the shear gradient direction are sliding or slipping planes in the steady shear flow, while a BCC twin structure is generated with {110} layers normal to the shear gradient. By further increasing the shear rate, shear melting finally takes place where the crystalline regularity is diminished. The shear orientation of the block copolymer micelles is recently applied to produce a template for arrangement of nanoparticles [21]. Effects of applying shear fields on the block copolymer cubic micelles are summarized significantly in some articles [16–18], which cover the cases of hexagonally-close packed rod micelles as well. Generally, rods or cylinders align parallel to the shear flow with $\{10\bar{1}0\}$ layers normal to the shear gradient [16,22]. As an industrial application, a significant technical advance was attained by Angelescu et al. [23], who performed macroscopic orientation of cylinders in a single layer film by applying shear flow. Since it is not straightforward to apply shear deformation on a thin film, they prepared a homemade sophisticated shearing apparatus. Application of simple shear flow on a double-gyroid structure has been conducted [24] but not thoroughly. Within a limited experimental variation, it was found that the double-gyroid structure underwent transformation to the hexagonally-close packed cylinders which align parallel to the shear flow with $\{10\bar{1}0\}$ layers normal to the shear gradient. Although it was failed to orient the double-gyroid structure using the shear flow, this unfavorable result may not be a final conclusion as taking into account of the success in the macroscopic orientation of the double-gyroid structure using a roll cast technique (which will be mentioned later). The failure of the orientation of the double-gyroid by the shear flow in the literature [24] may be ascribed to a limited experimental variation examined. More experimental exploration in wide parameter ranges should be required. As a matter of fact, Vigild et al. [25] have succeeded in preparing well-aligned gyroid structures by applying the large-amplitude oscillatory shear (LAOS), although experimental details were not available in the article.

As for the lamellar orientation by shearing, there are a bunch of reports and therefore it is difficult to cover them thoroughly. Refer to some excellent review articles [15–18]. Here, I briefly summarize directions of the lamellar orientation with respect to the applied shear. Fig. 1 shows schematics of ordered lamellar microdomains in the orthogonal coordination with 1 ($\mathbf{v}$): velocity (or shear) direction, 2 ($\nabla\mathbf{v}$): velocity gradient direction, and 3 ($\mathbf{v}\times\nabla\mathbf{v}$): vorticity direction. The orientation with the lamellar normal parallel to 2 is referred to as "parallel" orientation (a), parallel to 3 as "perpendicular" orientation (b), and parallel to 1 as "transverse" orientation (c). Either "parallel" or "perpendicular" orientation can be accessed by shearing [26,27]. On the other hand, the "transverse" orientation is believed to be "forbidden". However, one can find some publications reporting the "transverse" orientation [28–31], although it seems to be non-equilibrium. Okamoto et al. have reported coexistence of "parallel" and "transverse" orientations under LAOS, while Pople et al. [29] found it under steady shear flow. The latter case involves transition to "perpendicular" orientation by increasing the shear rate. In these studies diblock copolymer samples were utilized. On the contrary, the "transverse" lamellae were produced as kinetically-frozen structures [30,31] using pentablock copolymers. This can be referred to as chain architecture mediated. Vigild et al. [30] have reported that shear-induced disordered state under LAOS exhibits anisotropic feature in the concentration fluctuation, where the fluctuation is considerably intense in the sharing direction. This may be associated with the feature of the chain architecture of the pentablock where the linear alternation of chemically-different moieties may play an important role. With sudden cessation of the shear, the disordered system with the anisotropic fluctuation undergoes microphase separation and

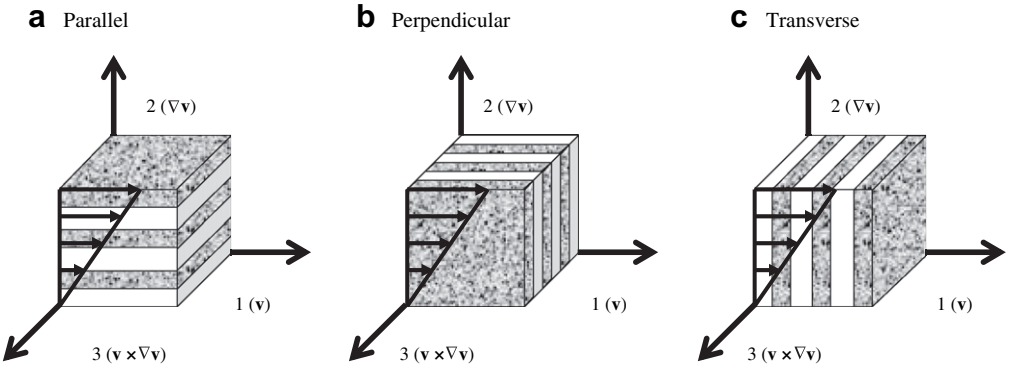

Fig. 1. Schematics of ordered lamellar microdomains in the orthogonal coordination with 1 ($\mathbf{v}$): velocity (or shear) direction, 2 ($\nabla\mathbf{v}$): velocity gradient direction, and 3 ($\mathbf{v}\times\nabla\mathbf{v}$): vorticity direction. The orientation with the lamellar normal parallel to 2 is referred to as "parallel" orientation (a), parallel to 3 as "perpendicular" orientation (b), and parallel to 1 as "transverse" orientation (c).

results in the formation of lamellae of which alternation exists only in the shear direction, giving rise to the "transverse" orientation. Similar situation may be expected in case of the solution extrusion of the pentablock copolymer, where Harada et al. [31] found the formation of lamellae with "transverse" orientation. More interestingly, they have succeeded in creating hexagonal-close packing of cylindrical microdomains with "transverse" orientation by inducing thermotropic morphological transition to cylinders from the lamellae with "transverse" orientation.

Okamoto et al. [28] applied LAOS to a bulk SEP (polystyrene-*block*-polyethylenepropylene) diblock copolymer having randomly-oriented and strongly-segregated lamellae. Although the "parallel" orientation is dominant, the "transverse" orientation coexisted. It was impossible to obtain perfect "parallel" orientation. To account for co-existence, kink band formation [32,33] can be a candidate of the model. The orientation of lamellae in the kink bands is inclined whereas the surrounding matrix contains almost perfect parallel lamellae. Shear-induced lamellar rotation observed by Polis et al. [32] has been considered as a consequence of the kink bands growth [33].

As mentioned above, lamellae composed of pentablock copolymers have interesting aspects in orientation owing to its feature in the chain architecture [34]. The parallel orientation of the lamellae has been considered to be unfavorable as compared to the perpendicular orientation because of the bridge conformation of middle block chains both in A and B lamellar phases, which resist against deformation in the parallel orientation [34]. On the contrary, the loop conformation of middle block chains or the dangling conformation of end block chains in the lamellar phase can allow slip within the lamellar space so that the parallel orientation can be allowed in the shear deformation. However, it might be rare for all of the middle chains of the pentablock copolymers to take the loop conformation. Thus, the parallel orientation of lamellae composed of the pentablock copolymers has been believed to be forbidden [30]. On the contrary, this unfavorable situation is not serious in case of triblock copolymers and is trivial in case of diblock copolymers, where the bridge conformation exists only in a lamellar phase of a middle block component in the former case and no bridge conformation in the latter case.

Nevertheless, Wu et al. [35] have shown evidence of the parallel orientation of lamellae in pentablock copolymers by conducting LAOS at the large deformation (high amplitude) and proven that the parallel orientation can minimize chain stretching by forming slip zone in the lamellar space with the predominant loop conformation. Namely, it may be considered that almost all of the middle block chains take the loop conformation even for the pentablocks.

This amazing result reminds us the importance of the way of applying shear: dynamic or steady shear. The former category involves the LAOS technique where the lamellar orientation depends not only on frequency but also the strain amplitude. While frequency dependence has well been known [36–38], strain amplitude dependence has been also noticed [34]. The former researches have documented the perpendicular orientation at small frequency and parallel orientation at high frequency. The latter researches also commented the importance of thermal history by showing their experimental result that the orientation is opposed depending on thermal history. Namely, a poly(cyclohexyl-ethylene)-*block*-polyethylene-*block*-poly(cyclohexyl-ethylene) triblock copolymer sample displayed very peculiar orientation behavior when the LAOS technique was applied to the sample having lamellar microdomains or to the sample in the disordered state (without forming lamellar microdomians). For both cases, almost perfect parallel orientation was observed by imposing LAOS with the smallest strain. However, further dependency was quite different by increasing the strain amplitude; biaxial orientation (parallel and perpendicular) was obtained with the fraction of the perpendicularly-oriented lamellae being monotonically increased when LAOS was imposed on the sample in the disordered state. As for the initially-ordered sample, almost perfect perpendicular orientation was suddenly attained by slightly increasing the strain amplitude from the smallest strain value and the fraction of the perpendicularly-oriented lamellae gradually decreased with further increasing the strain amplitude. This complicated behavior has been explained by viscoelastic contrast between the block components and their nonlinear stretching, each of which operates differently on the initially disordered and ordered samples.

Comprehensively, Maring and Wiesner [39] summarized orientation behavior in the diagram of a frequency–amplitude plot for LAOS of polystyrene-*block*-polyisoprene diblock copolymer lamellae in the vicinity of the order–disorder transition temperature (T_{ODT}). There are three regimes of orientation, which are "parallel", "perpendicular", and another "parallel" orientations. For the fully large strain amplitude, the manner of orientation merely depends on the deformation frequency; the order of the regimes is "parallel" (regime-A) → "perpendicular" (regime-B) → again "parallel" (regime-C) with an increase of the frequency. They commented that the "parallel" (regime-A) in the lower frequency region and the lower critical frequency between the parallel (regime-A) and perpendicular (regime-B) has not been deeply investigated so that more work is required. For the small strain amplitude, on the other hand, the orientation manner can be altered by increasing the strain amplitude; parallel (regime-A) for the lower strain values whereas perpendicular (regime-B) for the higher strain values. Thus, the boundary between these regimes A and B in the diagram is inclined in the small strain amplitude region. As for the case of lower temperature far from the T_{ODT}, the perpendicular orientation was hardly seen; actually it was not observed at very low temperatures, namely perfect parallel orientation was always obtained.

Kinetics of the lamellar reorientation has been studied by Wang et al. with the two-dimensional small-angle neutron scattering (2D-SANS) in-situ experiments [38,40]. Upon transformation from perpendicular to parallel orientation, undulation instability of lamellae takes place, followed by the buildup of parallel lamellae. This mechanism is referred to as *grain rotation*. They have further found that the kinetics of conversion of perpendicular to parallel lamellae are surprisingly slow, may be many orders of magnitude longer than the molecular relaxation time. However, the quality of alignment obtained was much better than that obtained in case of imposing shear on the disordered sample. Therefore, the results also suggest the importance of choosing the optimal thermal history (shearing on the ordered sample or on the disordered sample) and shear conditions (shear rate, frequency, strain amplitude) as well as shear mode (dynamic or steady shear) for obtaining defect-free samples in a limited amount of time. It was furthermore commented that samples prepared under suboptimal conditions contain defects being not easily annihilated by large-amplitude shear flow [40]. Thus the biaxial lamellar orientation (parallel and perpendicular) above-mentioned can be considered to be a transient state upon the lamellar reorientation.

We are now in a position to feature another selected method. That is a method imposing flow to the solution, where in the meantime the solvent keeps evaporating. This method is referred to as a *roll casting* [11–13,41–45]. Fig. 2 shows schematic views of the apparatus for the roll casting [11,42]. The casting solution is placed between two parallel rollers counter-rotating at a fixed gap being maintained by a micrometer. This apparatus allows free evaporation of solvent, therefore, effective force fields can be applied at a certain concentration of the casting solution, where chain entanglements are not so heavy in the microphase-separated structures due to remaining solvent. The advantages over the other methods can be recognized as follows: no thermal degradation is

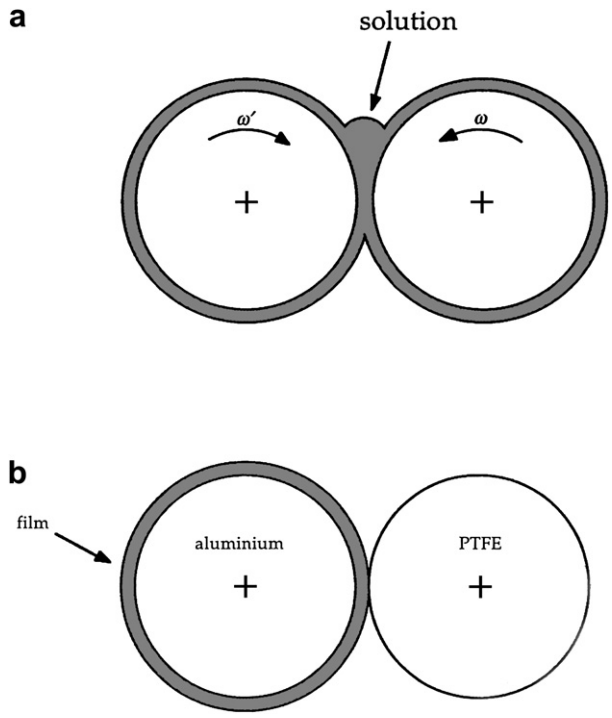

Fig. 2. Schematic views of the apparatus for the roll casting. (a) The casting solution is placed between two parallel rollers counter-rotating at a fixed gap being maintained by a micrometer. (b) When the solvent is completely evaporated, a cast film is made exclusively on an aluminum roller while no film is remained on a polytetrafluoroethylene roller. Adopted from Ref. [42].

encountered, resulting films are quite large (e.g., 20 cm × 6 cm × 2 cm), the time required for completeness of the microdomain orientation is much shorter (less than an hour), and a large number of variables can be changed individually, which enables us to find the most appropriate experimental condition by sample to sample. Thomas and colleagues successfully aligned not only cylinders [11–13,41,42,44] and lamellae [41] but also spheres [43] or double-gyroid strucutures [45] on a ⟨111⟩ crystallographic direction parallel to the flow direction.

3. Electric fields

Serpico et al. [46] have clearly presented that cylindrical microdomains evolved parallel to the applied electric fields in a blend of polystyrene homopolymer and polystyrene-*block*-poly(ethylene oxide) (PS–PEO) diblock copolymer when cast from solution in the presence of the electric fields. As for the melt of block copolymers, the lamellar microdomains have been found to orient parallel to the electric fields [11,47–55] when the disordered melt was cooled down below T_{ODT} in the presence of the electric fields. It has been also found that cylindrical microdomains in the melt align parallel to the electric field [51–53]. In principle, microdomain orientation is ascribed to difference in the dielectric constants for the constituent block components. Amundson et al. [48] have shown a theoretical treatment of the microdomain in the electric field. For a dielectric material in the electric field, the free energy is given as

$$F = F_0 - \frac{1}{8\pi}\int_V \varepsilon(\boldsymbol{r})|E(\boldsymbol{r})|^2 \mathrm{d}^3\boldsymbol{r} \tag{1}$$

where F is the free energy and F_0 the free energy without an electric field, $\varepsilon(\boldsymbol{r})$ the local dielectric constant, and $E(\boldsymbol{r})$ the electric field. The integration is conducted over the volume of the material, V. The block copolymer microphase separation causes a spatial modulation (pattern) of the local composition $\psi(\boldsymbol{r})$, which can be a compositional order parameter, and hence the dielectric constant, $\varepsilon(\boldsymbol{r})$, is accordingly patterned. As a consequence, the free energy is altered. This indicates that the free energy is a functional of the order parameter $\psi(\boldsymbol{r})$. Therefore, to formulate the free energy it is required to express the dielectric constant $\varepsilon(\boldsymbol{r})$ as a function of the order parameter $\psi(\boldsymbol{r})$. For this purpose, Amundson et al. have introduced the power-series expansion of $\varepsilon(\boldsymbol{r})$ with respect to $\psi(\boldsymbol{r})$ up to the second order,

$$\varepsilon(\boldsymbol{r}) = \varepsilon_D(\boldsymbol{r}) + \beta\overline{\psi}(\boldsymbol{r}) + \frac{1}{2}\frac{\partial^2\varepsilon}{\partial\psi^2}[\overline{\psi}(\boldsymbol{r})]^2 \tag{2}$$

where β denotes the sensitivity of the dielectric constant upon the change in the order parameter ($\beta = \partial\varepsilon/\partial\psi$), and the dielectric constant $\varepsilon(\boldsymbol{r})$ is assumed to be homogeneous, i.e., $\varepsilon(\boldsymbol{r}) = \varepsilon_D$, in the case of zero-th order parameter ($\psi(\boldsymbol{r}) = 0$). Finally, the free energy F arrives at

$$\frac{F - F_0}{V} = \frac{1}{8\pi}\varepsilon_D|E_0|^2\left[\left(\frac{\beta}{\varepsilon_D}\right)^2\left\langle\overline{\psi}^2\right\rangle(\mathbf{e}_q\cdot\mathbf{e}_z)^2 - \frac{\langle\varepsilon\rangle}{\varepsilon_D}\right] \tag{3}$$

where $\mathbf{e}_q$ and $\mathbf{e}_z$ are the unit vectors of the lamellar normal and that in the direction of the electric field, respectively. $\langle\varepsilon\rangle$ stands for the space-averaged dielectric constant.

To examine the effects of the electric fields, Amundson et al. [49] have shown the following scheme through the Landau free energy density. Getting started with a compositional order parameter variation in the ordered phase, which is expressed by the sinusoidal modulation as

$$\overline{\psi} = 2A\cos(q\times\mathbf{e}_q\cdot\boldsymbol{r}) \tag{4}$$

where A is the amplitude and q is the wavenumber, the Landau free energy $f(A)$ is written by

$$f(A) = \rho_c k_B T\left(\tau_R A^2 + \frac{u_R}{4}A^4 + \frac{w_R}{36}A^6\right) \tag{5}$$

where ρ_c is the number density of the polymer chains, k_B the Boltzmann's constant, T the absolute temperature. τ_R, u_R, and w_R are renormalized thermodynamic coefficients, which are related to χN, with χ and N being the Flory–Huggins interaction parameter per segment and number of the segments in a polymer chain, respectively. In the electric field, the free energy is increased as given by Eq. (3) so that the Landau free energy density of the second-order amplitude term is modified as

$$f(A) = \rho_c k_B T\left[(\tau_R + \eta_{elec})A^2 + \frac{u_R}{4}A^4 + \frac{w_R}{36}A^6\right] \tag{6}$$

where η_{elec} is an electric field energy per volume of a polymer chain in the unit of k_BT, as

$$\eta_{elec} = \frac{1}{4\pi}\frac{\left[\left(\beta^2/\varepsilon_D\right)(\mathbf{e}_q\cdot\mathbf{e}_z)^2 - (1/2)\left(\partial^2\varepsilon/\partial\psi^2\right)\right]|E_0|^2}{\rho_c k_B T} \tag{7}$$

Fig. 3 shows the Landau free energy as a function of the amplitude for a given q. The curve (a) is for the system in the disordered state, the curve (b) is for the system just at the order–disorder transition (ODT), and the curve (c) is for the system in the ordered state. The cases without application of the magnetic field are shown with solid curves. When the electric field is applied in the ordered state, the curve (c) changes the shape into that drawn with the broken line. Note here that the local minimum at $A = 0$ with $f(A) = 0$ does not change, while the free energy of two minima at nonzero A values becomes slightly larger. Although it is not explicitly discussed in Ref. [49], the values of A at the minima seem to shift towards zero ($A \to 0$). Note also that the increase of the free energy and the shift of the amplitude depend on the lamellar orientation

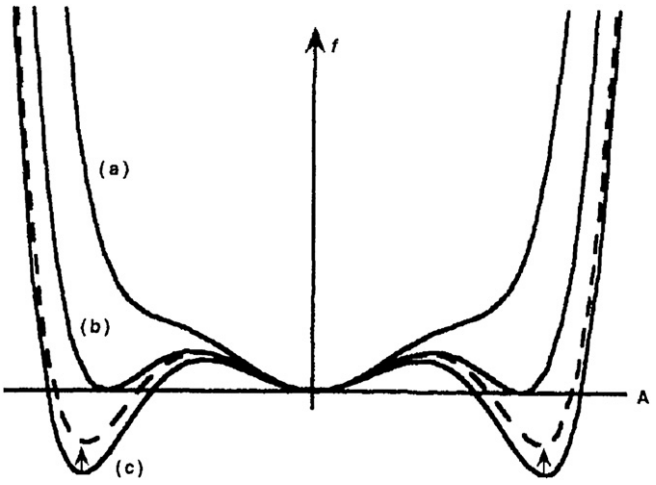

Fig. 3. The Landau free energy as a function of the amplitude for a given q. (a) is the case when the system is in the disordered state, (b) is just at the order–disorder transition, and (c) is in the ordered state. Those are shown with solid curves for the case without applying the magnetic field. When the magnetic field is applied in the ordered state, the curve (c) changes the shape into that drawn with the broken line. Adopted from Ref. [49].

with respect to the applied electric field. These changes upon the application of the electric field imply the shift of the ODT temperature. In other words, the ODT will be more accessible in the direction parallel to the applied electric field. This might be a driving force of the lamellar orientation parallel to the applied electric field.

To examine the stability of lamellae which have two extremes of orientation, the contribution of η_{elec} to the thermodynamic stability limit has been considered:

$$(\chi N)_{\mathrm{ODT}} = 10.495 + 37.823N^{-1/3} + 0.79022\eta_{\mathrm{elec}} \quad \text{at composition} \quad \phi = 0.5 \tag{8}$$

where $(\chi N)_{\mathrm{ODT}}$ denotes the value of χN at T_{ODT}. This gives the difference in $(\chi N)_{\mathrm{ODT}}$ for lamellae with two extremes of orientation

$$\Delta(\chi N)_{\mathrm{ODT}} = (\chi N)_{\mathrm{ODT}}\big|_{\parallel} - (\chi N)_{\mathrm{ODT}}\big|_{\perp} = -0.062884\left(\beta^2/\varepsilon_{\mathrm{D}}\rho_{\mathrm{c}}k_{\mathrm{B}}T\right)E_{\mathrm{O}}^2 \tag{9}$$

Note here that $\Delta(\chi N)_{\mathrm{ODT}}$ is proportional to the square of the field strength, E_{O}^2. More recently, Gunkel et al. [55] have developed a similar approach by including the composition fluctuation, and have arrived at

$$(\chi N)_{\mathrm{ODT}} = 10.495 + 41.018N^{-1/3} - 0.29705\alpha \quad \text{at composition} \quad \phi = 0.5 \tag{10}$$

with $\alpha \cong \eta_{\mathrm{elec}}$ which is also proportional to E_{O}^2. This equation suggests that the electric field lowers $(\chi N)_{\mathrm{ODT}}$, which in turn indicates that the electric field favours microphase separation. However, this conclusion causes inconsistency with the same authors' another main conclusion of the effect of the electric field on the composition fluctuation. Actually, they have meanwhile shown the effect of the electric field on the amplitude, as

$$A_{\mathrm{ODT}} = 0.81469N^{-1/6} - 0.0071843N^{1/6}\alpha \tag{11}$$

which clearly indicates that the electric field shifts A at the ODT towards zero by the factor proportional to E_{O}^2, implying that the electric field suppresses the extent of microphase separation. It has also been mentioned in Ref. [55] that the fluctuation in the disordered state is suppressed only in the direction of the electric field, causing an anisotropic scattering (collective structure factor) pattern. Thus, there seems to be something wrong in Eq. (10).

Although the result from Eq. (10) has an opposite sign as compared to the result from Eq. (8), we will herewith compare the extent of the difference in T_{ODT} ($\Delta T_{\mathrm{ODT}} = T_{\mathrm{ODT}}|_{\parallel} - T_{\mathrm{ODT}}|_{\perp}$) upon the application of the electric field. By using parameters for polystyrene-*block*-poly(methyl methacrylate) (PS–PMMA) given in Ref. [55] at $T_{\mathrm{ODT}} = 181\ ^{\circ}\mathrm{C}$ in case of the absence of the electric field for $N \cong 331$, let us estimate ΔT_{ODT}. The parameters are as follows: $\varepsilon_{\mathrm{PS}} = 2.5$, $\varepsilon_{\mathrm{PMMA}} = 5.9$, $\beta = \varepsilon_{\mathrm{PMMA}} - \varepsilon_{\mathrm{PS}}$, $\varepsilon_{\mathrm{D}} = (\varepsilon_{\mathrm{PMMA}} + \varepsilon_{\mathrm{PS}})/2$, $\rho_{\mathrm{c}}N = 7.20 \times 10^{21}\ \mathrm{cm}^{-3}$, and $\chi = 0.012 + 17.1/T$. For the field strength of $E_{\mathrm{O}} = 400\ \mathrm{kV/cm}$ (this is below a critical value for the dielectric breakdown of many polymers [49]). From Eq. (8) $\Delta T_{\mathrm{ODT}} \cong 6.5\ \mathrm{K}$ and Eq. (10) gives $\Delta T_{\mathrm{ODT}} \cong -2.5\ \mathrm{K}$ [55]. Although it is unclear that the difference in these values can be directly ascribed to the effect of the composition fluctuation, further experimental confirmation deserves a future work.

It might be a shortcoming that the microdomain reorientation by the electric field is slow and takes time. To overcome this problem, it is usually conducted cooling down the sample across T_{ODT} from disordered melt. It has been reported in Ref. [53] that composition fluctuations were oriented in the disorder melt in the presence of the electric field and then cylinders with parallel orientation were evolved upon cooling down the sample across T_{ODT} from the disordered state. As for the case when starting from the ordered cylinders perpendicularly oriented to the electric field, the reorientation occurs by the electric torque acting on a small grain, which is in advance resulted by local dissolution of the microdomains, especially in the vicinity of the grain boundary, reducing the grain size. For a lamellar sample, the similar mechanism was reported in Ref. [54] and lamellae with parallel orientation was reported to be very quick such that it was completed within minutes, as revealed by in-situ SAXS (small-angle X-ray scattering).

In Ref. [49] the mechanism of microdomain reorientation in the electric fields has also been discussed based on their theoretical considerations. Two of them were considered, (i) alignment by selective orientation and (ii) defect annihilation. The case (i) may be mostly relevant to the experiments cooling down the sample across T_{ODT} from disordered melt. As discussed above, there might be a difference in T_{ODT} for the parallel and perpendicular orientations in the presence of the electric field. Upon cooling from the disordered state, the orientation having higher T_{ODT} will be preferentially evolved. If a grain having this orientation grows up immediately, there will be no chance for a grain having other orientations to emerge. As a result, the favorable orientation prevails in the sample. On the other hand, the case (ii) is relevant to the microdomain reorientation upon application of the electric field in the ordered state. As discussed above, experimentally observed mechanism with the electric torque acting on a small grain is another candidate of the microdomain reorientation, which has not yet been theoretically considered.

4. Magnetic fields

As discussed above, the electric field is a promising way to control orientation of the microdomains. However, there is a crucial problem in this method, that is, the dielectric breakdown. This limits the applicability of the electric field for a thin film and puts a limitation to the field strength. As far as electromagnetics are concerned, similar effects are anticipated for magnetic fields. As the spatial modulation of the dielectric constant determines the free energy of the system in the electric field, that of the magnetic permeability determines the free energy in case of the magnetic field. Furthermore, the magnetic field has superiority in its applicability, because there is no concern of the dielectric breakdown. Namely, the film thickness is not necessarily thin, as far as the sample can be placed in a bore of a magnet. Of course, it is needless to state that there is a technological limitation of the strength of the magnetic field (due to an apparatus). At present, the world highest magnetic field, which should be maintained for at least several tens

of minutes, being required for a realistic thermal annealing to induce a magnetic orientation of microdomains, is around 35 T. Such a high magnetic field can be available by the use of a superconducting magnet settled in some of specific facilities [56].

The first report of controlling orientation of block copolymer microdomains appeared in 1998 [57] where a 2.4 T magnetic field was imposed on a diblock copolymer comprising both block chains of liquid-crystalline polymers (LCP). Preferential orientation of microdomains was observed by SAXS. Since mesogenic units of a liquid crystal can be easily aligned by the application of the magnetic field, the resultant microdomain orientation of the LCP–LCP diblock copolymer is not so striking. Several years later, Hamley et al. [58] have reported the difference in the extent of the microdomain orientation by the magnetic field in case of LCP–amorphous type diblock copolymers, where the amorphous part was polystyrene (PS), for two extreme cases of the LCP-phase cylinders in the PS matrix and the PS cylinders in the LCP matrix. They found preferential orientation of the LCP-phase cylinders by application of the moderate magnetic field of 1.8 T, while no orientation found in case of the PS cylinders in the LCP matrix. A higher magnetic field of 9 T was found to be required to align the PS cylinders in the LCP matrix [59], and soon later the magnetic field of 5 T was found to be enough for the orientation of the PS cylinders [60]. For the latter sample, the orientation mechanism was studied by SAXS and WAXS (wide-angle X-ray scattering) experiments [61]. Since it has been found that crystallites of a crystalline polymer can be aligned by the magnetic field [62–65] due to the anisotropy in the diamagnetic susceptibility of the crystalline lattice (as a consequence of the magnetic torque), this can be also applied for the microdomain orientation. Actually, it has been reported that crystalline lamellar structures were aligned perpendicular to the applied magnetic field of 7 T, using a poly(ethylene oxide)-*block*-polybutadiene (PEO–PB) crystalline–amorphous type diblock copolymer sample [66].

There has been no report on the magnetic orientation of the microdomains of amorphous–amorphous type block copolymers (i.e., neither LCP nor crystalline moieties which are responsible for the magnetic field), although it is expected from the analogy of the case of the electric field. One of the big difference between them may be that the contribution due to the spatial modulation of the magnetic permeability is trivial as compared to that of the dielectric constant. To overcome the difficulty for the magnetic orientation, enhancement of the extent of spatial modulation in the magnetic permeability will be effective. To check the effects, we have conducted selective doping of iron-containing chelate compounds in a particular phase which forms a cylinder [67]. The selective doping was conducted by the assistance of a selective solvent upon the solution casting. In the solution of the block copolymer with a selective solvent, solvent molecules are inhomogeneously distributed. Especially, they are accumulated in a phase having chemical affinity to the solvent. Since the chelate compounds are dissolved by the solvent, the chelate compounds are automatically accumulated in the phase having chemical affinity to the solvent, irrespective of the chelate compound nature, whether or not it directly has affinity to a particular component of the block copolymer. After complete evaporation of the solvent, the chelate compounds are consequently doped in the particular phase. This scheme was applied to the cylinder-forming polystyrene-*block*-poly(ethylene butylene)-*block*-polystyrene (SEBS) triblock copolymer solution in dichloromethane. After the solution cast, however, thermodynamically non-equilibrium morphology was formed, which was in this particular case the lamella. The lamellar microdomains were found to align parallel to the substrate much better when the cast was conducted in the magnet with 12 T. Then, we conducted thermal annealing of this sample at 190 °C in the magnet with 12 T (the direction of the applied magnetic field was parallel to the as-cast film and parallel to the substrate surface, as well) to induce transformation from the non-equilibrium lamellae into equilibrium cylinders. Finally, we have obtained well-ordered cylinders with the hexagonal-close packing, as shown in Fig. 4. Note here that cylinders are parallel to the applied magnetic field with a crystallographic plane $\{10\bar{1}0\}$ of the hexagonal lattice being preferentially parallel to the substrate. Upon the transformation of the non-equilibrium lamellae, the flat interface starts undulating, as schematically shown in Fig. 5, which causes a spatial modulation of the magnetic permeability. Due to the selective doping, the modulation causes excess free energy in the magnetic field. From the analogy of the electric field, it can be considered that the undulation of the lamellar interface perpendicular to the applied magnetic field costs more as compared to the undulation parallel to it. Thus, the parallel undulation is selected and as a consequence, the cylinders orienting parallel to the field emerged preferentially. We also found parallel orientation of cylinders without doping the chelate compounds, although the extent was much lesser.

When the magnetic field was applied perpendicular to the as-cast film upon the thermal annealing, no homeotropic orientation of the cylinders by the guidance of the magnetic field was attained. This result is very much contrast to the above-mentioned favorable result in the case of applying the parallel magnetic field, which implies that the effect of the substrate surface (or the free surface of the as-cast film) to lay down cylinders parallel to those surfaces is much larger than the effect of the magnetic field. To overcome the surface affirmative interaction, which obstructs the homeotropic orientation of the cylinders by the guidance of the magnetic field, a much higher field was required. Therefore, we conducted thermal annealing in the presence of a 30 T magnetic field [68]. For this particular case, thin films with thickness ranging from 20 nm to 300 nm were used to enable the AFM observation of the free surface of the film spin-cast on silicone wafer. The sample used is the cylinder-forming SEBS (the same sample as used in the above-mentioned study), but for this particular study the chelate compounds were not doped. Spin-casting toluene solutions on the silicone wafer, thin films were obtained, which was further subjected to thermal annealing in the 30-T magnetic field. Fig. 6(a) and (b) shows AFM results for a 20-nm thick film after free annealing (thermal annealing in the absence of the magnetic field at 180 °C for 12 h), a phase image and a corresponding height image from the tapping mode measurement, respectively. Fig. 6(c) and (d) is the AFM phase image for a 20-nm thick film annealed at 180 °C for 3 h in the presence of the 30-T magnetic field parallel and perpendicular to the substrate surface, respectively. As a comparison, Fig. 6(e) and (f) is for a 60-nm thick film and for a 300-nm thick film annealed at 180 °C for 5 h in the presence of the 30-T magnetic field parallel and perpendicular to the substrate surface, respectively. First of all, the cylindrical microdomains were obtained for the freely-annealed sample without any preferential orientation, as observed in Fig. 6(a) and (b). Therefore, the thermal annealing of the film in the presence of the magnetic field was intended to induce reorientation of the cylindrical microdomains. The annealing duration was 3–5 h and the annealing temperature was 180 °C. Note that the diameter of a cylinder is 13 nm so that for (c) and (d) the film thickness is comparable to the diameter of the cylinder. Fig. 6(c) shows a preferential orientation of the cylinders parallel to the direction of the applied magnetic field, while the panel (d) does not contain a patch of the homeotropic orientation of cylinders, although a reorienting cylinder is detected locally. It may be considered that the film thickness is too thin to overcome the surface affirmative interaction. It has been known that film thickness causes physical constraints on the formation and the orientation of the microdomain structures due to spatial confinement in thin films. Actually, Knoll et al. have experimentally shown changes in the orientation and the morphology as a function of the film thickness for cylinder-forming SBS (polystyrene-*block*-polybutadiene-*block*-polystyrene) triblock

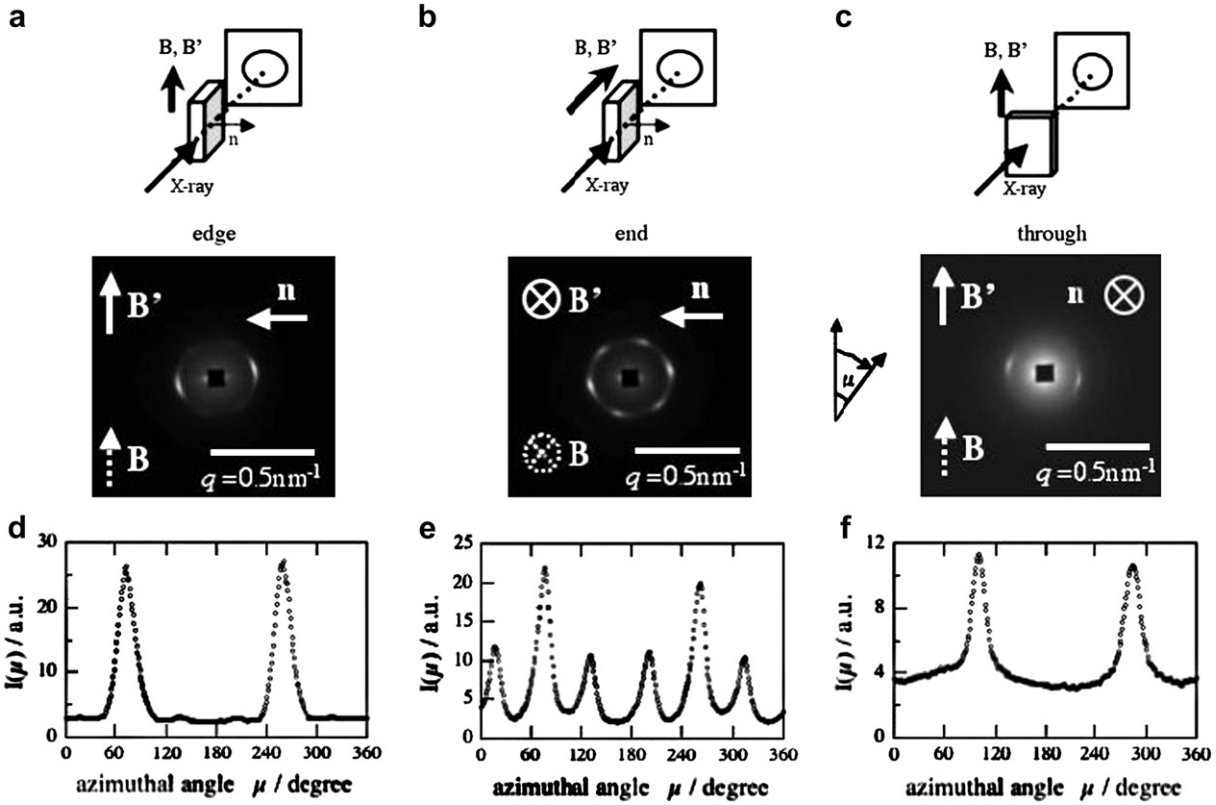

Fig. 4. An example of magnetic orientation of the microdomains of amorphous–amorphous type block copolymers (a 2D-SAXS pattern for hex-cylinders of PS (polystyrene) cylinders in polystyrene-*block*-poly(ethylene butylene)-*block*-polystyrene (SEBS) triblock copolymer). Iron-containing chelate compounds are selectively doped in a PS cylinder. The selective doping was conducted by the assistance of a selective solvent (dichloromethane) upon the solution casting. The solution cast and a successive thermal annealing at 190 °C were conducted in the 12-T magnet. The direction of the applied magnetic field is parallel to the as-cast film and parallel to the substrate surface, as well. Results of the 2D-SAXS measurements of the annealed film, which was annealed in the presence of the magnetic field. The original cast film before annealing was obtained by casting from the dichloromethane solution with the chelate. Panels (a), (b), and (c) are 2D-SAXS patterns, while panels (d), (e), and (f) are the intensity distributions as a function of the azimuthal angle μ for the 1st-order peak. Panels (a) and (d) are for the edge view, panels (b) and (e) are for the end view, and panels (c) and (f) are for the through view. Adopted from Ref. [67].

copolymers [69,70]. With an increase of the thickness, the change is as follows; disordered state → perpendicular cylinders → parallel cylinders (one layer of a cylinder array) → perforated lamellae → parallel cylinders with necks → again perpendicular cylinders → again parallel cylinders (but two layers of a cylinder array) → …. When the thickness is comparable to the diameter of the cylinder, parallel orientation is much preferred. In this situation, it is expected that perpendicular reorientation by imposing the vertical magnetic field is difficult, even though the magnetic field would have in principle an ability to align cylinders parallel to it. Therefore, our unfavorable result shown in Fig. 6(d) may suffer from such thickness constraint. Comparing Fig. 6(d) with Fig. 6(a), however, implies the effect of the magnetic field.

For a thicker film, the physical constraint due to film thickness is expected to decrease so that both parallel and homeotropic orientations of the PS cylinders are clearly seen in Fig. 6(e) and (f), respectively, for the directions of the applied magnetic fields parallel and perpendicular to the film (substrate) surface. It is expected that an increase of the film thickness is effective for overcoming the surface affirmative interaction. However, still concerns remain, that is, our AFM result revealed only the surface structure. As discussed in the following section of the surface field, there is a chance to obtain perpendicular orientation of cylinders in the proximity of the free surface by controlling the atmosphere surrounding the sample film even in case of thick films. To avoid misjudgment of the effect, it is required to understand correctly the behaviors of orientations in the film (the effect of the "surface field" will be thoroughly discussed in the following section). In our particular case, we have also conducted grazing-incidence small-angle X-ray scattering (GISAXS) measurements for all of those samples and results consistent with the AFM results were obtained, suggesting that over a wide region in the spin-cast film (not restrictedly in the surface area) the parallel or the homeotropic orientation prevails. It could be concluded that the cylinders in the interior of the films aligned parallel to the direction of the applied magnetic field (30 T).

By the analogy of the electric field, it is expected that the order–disorder transition temperature is different between two extremes of the cylinder orientations in the presence of the magnetic field, parallel or perpendicular to the direction of the applied magnetic field. A simple extension of the Clapeyron equation gives shift of a transition temperature due to the magnetic field as compared to a quiescent transition temperature [71].

$$\Delta T = \left\{\left(\cos^2\theta - 1/3\right)\chi_a + \langle\chi_S\rangle - \chi_\ell\right\} B^2 T_m/(2\mu_D \Delta H) \tag{12}$$

where T_m is a quiescent transition temperature (i.e., in the absence of the magnetic field), θ the orientation angle between the principal axis and the field direction, χ_a anisotropy in the diamagnetic susceptibility given by $\chi_a = \chi_\parallel - \chi_\perp$, with $\chi_\parallel$ and $\chi_\perp$ being the diamagnetic susceptibilities parallel and perpendicular to the principal axis, respectively. Furthermore, $\langle\chi_S\rangle$ and χ_ℓ are the average values of the diamagnetic susceptibility in the phase I and that in the phase II, respectively (supposed to be a solid phase and a liquid phase, respectively), B the magnetic flux density, μ_0 the magnetic permeability of a vacuum, ΔH the enthalpy change associated with the transition (enthalpy of fusion). For a melting temperature of

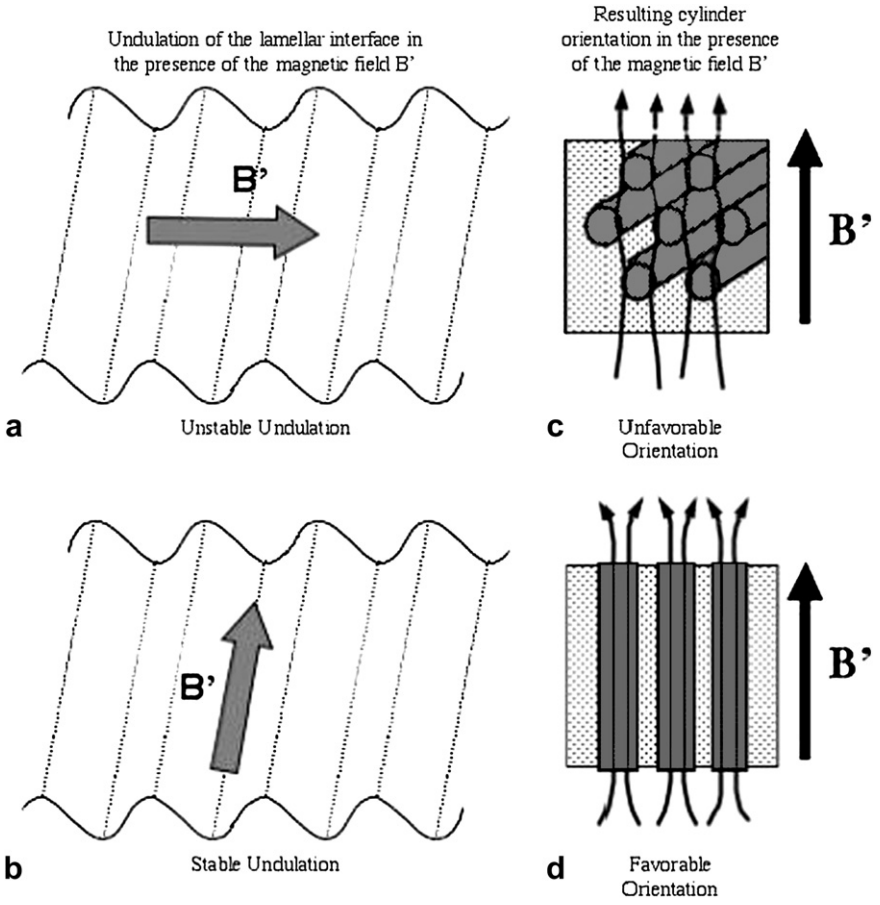

Fig. 5. Schematic illustrations for (a) unstable and (b) stable undulation modes of the lamellar interface, and (c) unfavorable and (d) favorable cylinder orientations in the presence of the magnetic field. The undulation of the lamellar interface is the key step for the transformation from lamellae to cylinders upon the thermal annealing. Adopted from Ref. [67].

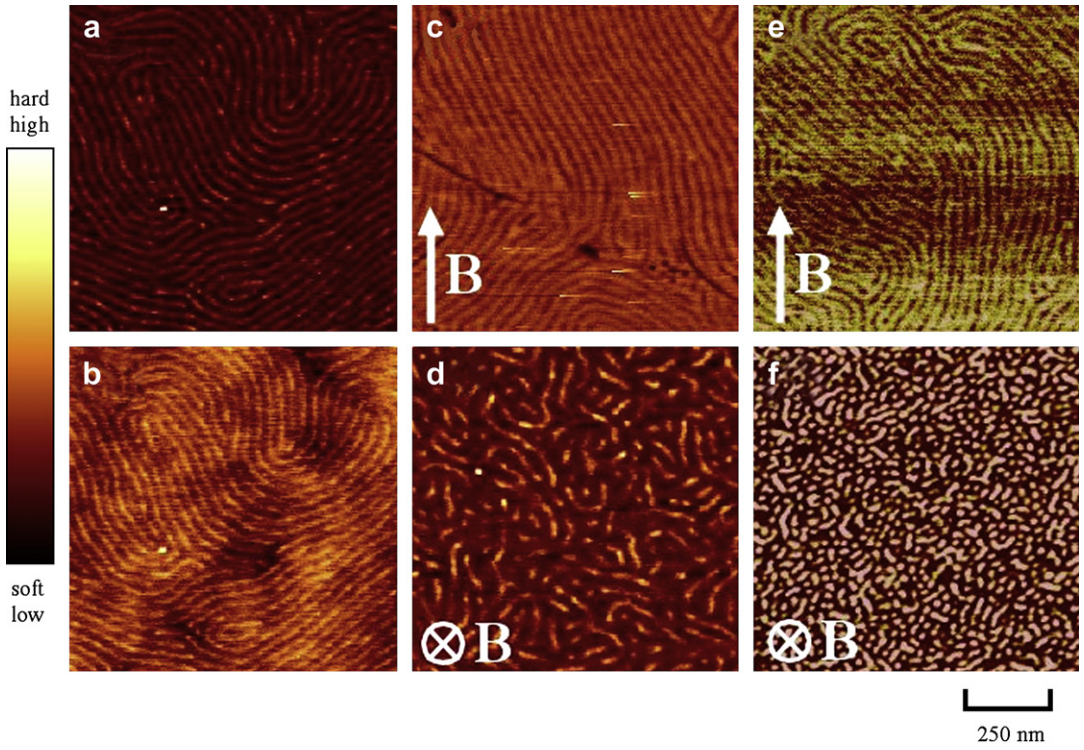

Fig. 6. AFM tapping mode images of a thin film (20-nm thick) annealed at 180 °C for 12 h in the absence of the magnetic field; (a) phase image and (b) corresponding height image. AFM tapping mode phase images of films annealed at 180 °C in the 30-T magnet; (c) 20-nm thick, annealed for 3 h in $B_{\parallel}$ (horizontal magnetic field), (d) 20-nm thick, annealed for 3 h in $B_{\perp}$ (vertical magnetic field), (e) 60-nm thick, annealed for 5 h in $B_{\parallel}$, and (f) 300-nm thick, annealed for 5 h in $B_{\perp}$. Adopted from Ref. [68].

water, it has been reported $\Delta T = 3$–20 mK for $B = 4$–6 T [72,73]. As for the block copolymer T_{ODT}, a comparatively large shift is expected from Eq. (12) since the enthalpy change associated with the ODT is quite small. We assume here that Eq. (12) can be extended to the discussion of T_{ODT} by reading θ as the orientation angle between the cylinder axis and the field direction, $\chi_{\parallel}$ and $\chi_{\perp}$ as the diamagnetic susceptibilities parallel and perpendicular to the cylinder axis, respectively. Furthermore, $\langle\chi_S\rangle$ and χ_ℓ read as the average values of the diamagnetic susceptibility in the ordered and that in the disordered phases, respectively ($\langle\chi_S\rangle = (\chi_{\parallel} + 2\chi_{\perp})/3$), and T_m and ΔH read as T_{ODT} and the enthalpy change associated with the ODT, respectively.

To evaluate the shift of T_{ODT}, we have conducted in-situ SANS experiments in the presence of a 10 T magnetic field for the cylinder-forming deuterated polystyrene-*block*-polybutadiene diblock copolymers (PS cylinders) [74]. As a result, it was found that the transition temperature was decreased by 0.15 °C with the 10 T magnetic field as compared to the case of no magnetic field. However, the difference is slightly larger than the experimental error associated with the accuracy of the temperature control so that we are not so confident with this result. The difference in T_{ODT} ($\Delta T_{ODT} = T_{ODT}|_{\parallel} - T_{ODT}|_{\perp}$) in the presence of the magnetic field is expected to be larger as compared to the difference in T_{ODT} with and without the magnetic field for the sample with random orientation. $\Delta T_{ODT} = \chi_a B^2 T_m/(2\mu_0 \Delta H)$, whereas $\Delta T = (\langle\chi_S\rangle - \chi_\ell) B^2 T_m/(2\mu_0 \Delta H)$, so that $\Delta T_{ODT} > \Delta T$ is expected if $|\chi_a| > |\langle\chi_S\rangle - \chi_\ell|$. Although $|\langle\chi_S\rangle - \chi_\ell| \cong 0$ is anticipated, $\chi_{\parallel}$ and $\chi_{\perp}$ (diamagnetic susceptibilities parallel and perpendicular to a cylinder axis, respectively) are unknown. Therefore, further quantitative discussion is not available. Note here that values of the mass susceptibilities are given for some of polymers in the literature [75], as $\chi = -7.85 \times 10^{-9}$ m^3/kg for PS and $\chi = -8.87 \times 10^{-9}$ m^3/kg for polyethylene, although the degrees of crystallinity, on which the values of χ may depend, were not clearly indicated. The SANS experiments to evaluate the difference ΔT_{ODT} in the presence of the magnetic field are currently going for samples containing well-oriented cylinders.

To conclude, there will be a difference in T_{ODT} for the parallel and perpendicular alignments, which scales quadratically with the field strength, irrespective of the electric or the magnet field. Moreover, the force field is not an exceptional. Since there is no concern about the dielectric breakdown or mechanical breakdown (including rupture of microdomains), the magnetic field is the most promising way to easily detect the difference in T_{ODT} through increasing the field strength safely up to limitation of the facility (or apparatus).

5. Surface field

Surface-induced phase separation and propagation into far deep inside of the sample is a generally accepted concept for a nucleation-and-growth type mechanism of the global kinetics how the microdomains are prevailing in the interior of a bulk sample. Considering the control of the microdomain orientation, controlling the surface-induced phase separation is important for the case of thin films, while controlling the propagation is crucial for the case of bulk samples. The latter requires directional fields, which is the subject of the following section. In this section, we discuss thermodynamic control of the surface property through controlling a substrate property or an atmosphere. Recently, these physicochemical constraints are categorically referred to as surface fields. It has been reported that patterning the surface of the substrate either chemically [76] or topographically [77] can give rise, respectively, to perpendicular orientation of lamellar microdomains, or to switching of the lamellar orientations regularly in thin films. Even in thick films, a perpendicular orientation of lamellae was observed near the substrate surface, which was chemically patterned, as far as the mismatching of the patterned periodicity with the lamellar repeat distance (spacing) was less than about 10% [78]. Furthermore, the surface-directed perpendicular orientation of lamellae continued up to about 500-nm depth from the substrate surface [78], which is comparable to the case of cylinders parallel to the surface up to about 200-nm deep [79]. This finding ensures that controlling of substrate surface property or an atmosphere is enough for controlling the overall orientation in thin films.

So-called "solvent annealing" or "solvent vapor treatment" [69,70,80–83] is a method of controlling the nature of the surface field. The surrounding atmosphere of the free surface of the polymer film, which is undergoing thermal annealing, or the surrounding atmosphere of the surface of the casting solution is filled with vapor of solvent, so that the atmosphere can be either neutral or selective to a particular component of the block copolymer.

The effects of the surface field are balanced with physical constraints due to the film thickness in case of thin films, resulting in different orientations and different morphologies depending on the film thickness [69,70]. The effect is not ascribed to the glass transition, in other words chain mobility, as realized by the experimentally observed fact that the well-ordered cylinders in a thin film was not obtained in the as-spin cast film even for the cast temperature being enough high as compared to the glass transition temperature of the components of the block copolymer [79]. Further thermal annealing at elevated temperature was required to attain better orientation of the cylinders which are parallel to the film surface. Note here that the parallel cylinders were formed in the interior with a wetting layer at the free surface for this particular case [79]. As discussed above, Knoll et al. have experimentally shown changes in the orientation and the morphology as a function of the film thickness for cylinder-forming SBS triblock copolymers [69,70]. With an increase of the thickness, the change is as follows, disordered state → perpendicular cylinders → parallel cylinders (one layer of a cylinder array) → perforated lamellae → parallel cylinders with necks → again perpendicular cylinders → again parallel cylinders (but two layers of a cylinder array) …. Variations of the microdomain structures with the strength of the surface field have been studied by simulations in the context of the mean-field dynamic density functional theory [84]. The phase behavior of cylinder-forming ABA triblock copolymers in thin films was modeled in detail. Some of the results are briefly summarized here.

Figs. 7 and 8 show simulated results exhibiting effects of the strength of the surface field for thick films and thin films, respectively. The composition of the polymer is $A_3B_{12}A_3$ for both cases. The parameter ε_M controls the strength, which is defined by $\varepsilon_M = \varepsilon_{AM} - \varepsilon_{BM}$ with ε_{AM} and ε_{BM} being the segmental repulsive interaction energy associated with contact between A segment and the surface, and that between B segment and the surface, respectively. By increasing ε_M, the repulsive interaction between the A segment and the surface increases over the B segment, so that the B segments become selectively favoring the surface. As for Fig. 7, the thickness corresponds to approximately 9 layers of a cylinder array. For most of the cases the microdomain structure remains hexagonally ordered cylinders aligned parallel to the surface, while near the surface the strucuture is different from the bulk one, depending on the field strength. This effect is referred to as the surface reconstruction and has been experimentally observed. For $\varepsilon_M < 2$, the A component forms wetting layer. When the surface field is neutral, perpendicular orientation is attained, which is seen for $2 < \varepsilon_M < 4$. From the fact that a neutral surface appears at the positive ε_M, which means energetically the A components unfavor the surface, entropic attraction of the shorter A chains to the surface can explain the neutral surface even for the positive ε_M by compensation of energetically unfavorable condition. With a further increase of ε_M, the A component becomes more unfavorable to the surface so that the surface structure shows parallel orientation of

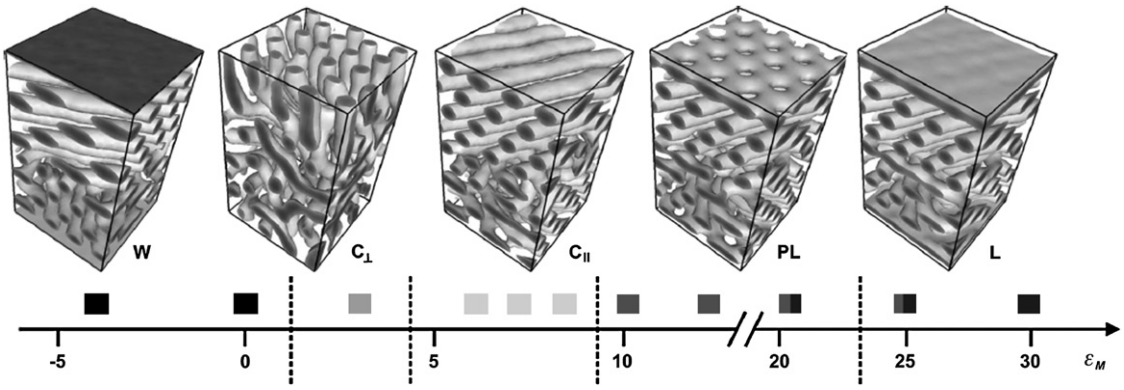

Fig. 7. Simulated results exhibiting effects of the strength of the surface field for thick films (the thickness corresponds to approximately 9 layers of a cylinder array). The composition of the polymer is $A_3B_{12}A_3$ for cylindrical microdomains. The parameter ε_M controls the strength, which is defined by $\varepsilon_M = \varepsilon_{AM} - \varepsilon_{BM}$ with ε_{AM} and ε_{BM} being the segmental repulsive interaction energies associated with contact between A segment and the surface, and that between B segment and the surface, respectively. Adopted from Ref. [84].

cylinders with B wetting layer. And further, perforated lamellae with B wetting layer, finally parallel orientation of a lamella is formed. Fig. 8 shows the results for a thin film with the thickness comparable to the diameter of a cylinder. The variation of the structure with ε_M is almost the same as the surface reconstruction seen in Fig. 7. However, it is noted that the disordered state is found in the case of the thin film. Although $\varepsilon_M \sim 3$ for the neutral surface is the same, ε_M at the border between the structures are much lower as compared to those found for a thick film (Fig. 7). This may be due to duplicated influence of the surface from both sides (top and bottom surfaces) in case of the thin film. Finally, it is noteworthy that experimentally observed spontaneous perpendicular orientation in thin films [4,9,10,85] can be now ascribed to the surface field with neutral condition, although in these experiments the atmosphere was not explicitly controlled.

To invoke perpendicular orientation of cylinders in thin films, the physical constraints due to film thickness should be removed as well as the neutralization of the atmospheric condition. Upon considering tactics for removal of the constraints, there is an interesting report; simply adding homopolymers into a matrix phase was found to be effective for the perpendicular orientation of cylinders [9]. In this report, the influence of the added homopolymers was explained as follows. In case when the homopolymers are not completely mixed with the corona block chains, i.e., the longer block chains which comprise the matrix phase, they are going to be localized in the corners of the Wigner–Seitz (WS) cell for the hexagonal lattice. Here, the WS cell defines the territory that should be filled with the corona chains anchoring to a cylinder which places at the center of the WS cell [86,87]. Since the corner is most distant from the center (or from the interface of the cylinder), the corona chains subjected to fill up the space near the corner should be mostly elongated and in turn mostly frustrated. Upon the addition of the homopolymers which are localized in the corner region of the WS cell, the frustration of the corona chains is almost removed. Kitano et al. [9] discussed that such an effect of adding homopolymers into the matrix phase can cause thermodynamically secured orientation, which is the perpendicular orientation of cylinders in this particular case. Although further experimental confirmation of the mechanism should be required, this phenomenon is ascribed to a consequence of the removal of the physical constraints owing to film thickness.

6. Directional fields

As identified above, a directional field is necessary to control overall orientation of microdomains in the interior of the film. Thus, we will discuss how to invoke directional fields from self-organizing block copolymer systems in this section.

Directional solidification occurs when the disordered melt is subjected to temperature gradient by moving it across the zone-

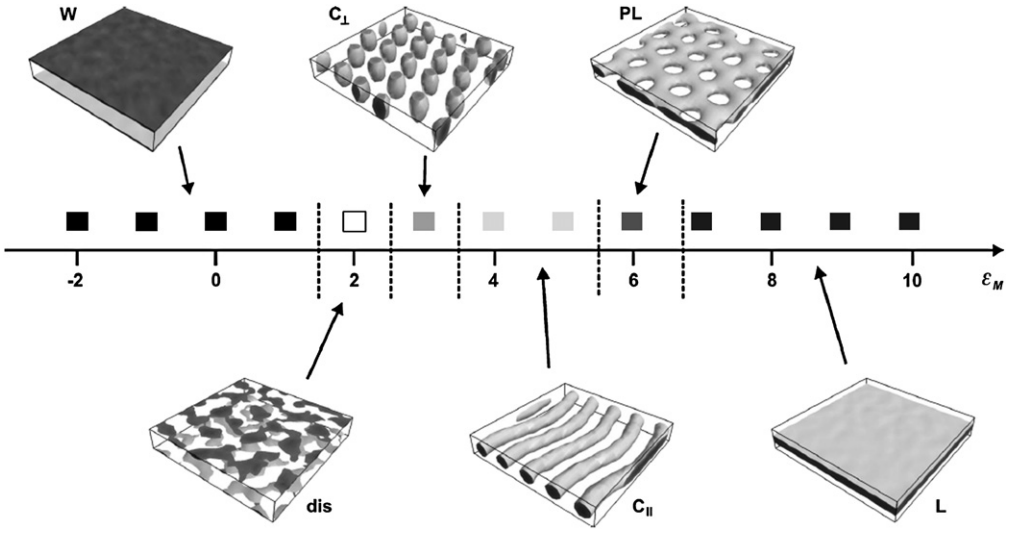

Fig. 8. Simulated results exhibiting effects of the strength of the surface field for thin films (the thickness comparable to the diameter of a cylinder). The other parameters are the same as those for Fig. 7. Adopted from Ref. [84].

heating device [88,89]. As a consequence, a single grain of lamellae was obtained with the lamellar normal parallel to the direction of the temperature gradient [89]. Directional eutectic solidification has been proposed by DeRosa et al. [6] using crystallizable solvent. When eutectic liquid (a block copolymer solution in the crystallizable solvent) underwent the solvent crystallization, ordered lamellae were then formed, which were overwhelming the solvent crystal with lamellar orientation perpendicular to the crystal surface and parallel to the solidification direction in thin films. In this case, the crystallization of the solvent guides the successive orientation of the lamellar microdomains. Both of the methods mentioned above are intended explicitly to invoke the directional solidification. On the contrary, there observed spontaneous occurrence of a directional solidification as a result of receding solution meniscus upon solvent evaporation during solution cast [90]. In the vicinity of the wall of a container for a solution casting, due to shear between the casting solution and the wall, well-oriented cylinders were obtained with the cylinder axis perpendicular to the receding direction of the solution meniscus. The microphase separation takes place at the meniscus and then propagates into interior of the solution. The authors also found that the double-gyroid structure can be aligned with a ⟨111⟩ crystallographic direction perpendicular to the receding direction. Here, solvent evaporation rate is one of the most important parameters for controlling the orientation and ordering of the microdomains.

Jeong et al. [91,92] have conducted an approach very similar to that of Kitano et al. [9] and then obtained perpendicular orientation of cylinders in thin films (up to about 330 nm thick). The big difference in the two methods lies in the quite opposite tactics that Jeong et al. added homopolymers inside of the cylindrical microdomains, not in the matrix phase. They found that a better perpendicular orientation of cylinders was attained when the added homopolymers are more localized in the core region of a cylinder. As a possible mechanism, they explained that the embedded homopolymer guides subsequent assembly [92]. In other words, if the homopolymers' core region grows preferentially straight, an ordering front can be formed. Therefore, the successive migration of the block copolymer chains results in the initiated perpendicularly-oriented cylinders near the free surface, if any, growing down (or up) into the interior of the film. Although further confirmation of the mechanism is required, this phenomenon reminds that the localization of the homopolymers can induce a directional field.

As observed in Fig. 7 for thick films, perpendicular orientation of cylinders can be seen near the surface of the film [84]. Similar phenomena were observed experimentally [93] for the as-cast sample being prepared by the rapid solvent evaporation. Although similar influences of the casting solvents may result in the perpendicular orientation near the free surface of the as-cast thick film, it is rather ascribed to a directional field caused by solvent evaporation. Actually, it has been reported for the case of thick films [93] and for the case of thin films [94], as well, that the rapid evaporation results in the perpendicular orientation of cylinders and lamellae, while the slow evaporation gives parallel orientation of them. On the other hand, if the solvent evaporation is very fast, either poor microphase separation or incompleteness of the perpendicular orientation is resulted [95]. Such incompleteness is due to limitation of time imparted for the microphase separation during the solvent evaporation. This fact implies that the solvent evaporation with an appropriate evaporation rate can induce a directional field. As the solvent evaporates, concentration gradient is induced such that the polymer concentration at the free surface of the solution is higher than that in the interior. As a consequence, microphase separation will take place at the surface of the solution, then it will grow down towards the interior, as depicted in Fig. 9. The directional solidification perpendicular to the film or solution surface proceeds with an ordering front parallel to the surface [93,96,97]. More detailed illustrations shown in Fig. 10 give a molecular picture of how the solvent molecule evaporates. Fig. 10 compares situations when the top surface of the polymer solution is covered with the ordering front of perpendicular lamellae or parallel lamellae. In the latter case, the covering layer significantly blocks the solvent migration, if the solvent mobility in microdomain A much differs as compared to that in microdomain B. The situation in the polystyrene-*block*-polybutadiene (PS–PB) block copolymer is the case. Therefore, perpendicular orientation will be initiated at the top surface of the solution for the case of a comparatively rapid solvent evaporation. Fig. 10 also explains how the ordering front proceeds; block copolymers still dissolved in the solution below the ordering front should be supplied from the solution phase to the ordering front. If the diffusion process would be translational as depicted in Fig. 10, the diffusion for the case of the parallel orientation is more hindered, as compared to the case of the perpendicular orientation. And then at the ordering front, incorporation of the supplied block copolymer chain would pay a more energetic cost in case of the parallel orientation. Thus, upon proceeding of the ordering front, the perpendicular orientation is favored. Although such a deterministic discussion for the growth of the front was made in Ref. [93], the difference may be trivial, because the diffusion should not be so simple as translational, but it is rather complex such as rotational-translation diffusion. For the explanation of the growth of the ordering front, the idea of the solvent permeation path given by Ho et al. [95] seems to be more appropriate. As the top covering layer becomes thicker, it is more crucial to retain the solvent permeation paths. This requirement can be a driving force of the perpendicular orientation more and more as the ordering front proceeds, irrespective of initial orientation in as-solidified top layer. Thus, the perpendicular orientation of lamellae or cylinders in thin films or in the proximity of the free surface of thick films can be explained.

Then what happens in the interior of the thick film. As can be seen in Fig. 7 [84], and in Refs. [78,93], it was theoretically and experimentally found that there is a limitation of the distance to which the surface-directed perpendicular orientation propagates. It is about 1 μm at most, which means that in the interior of the thick film, preferentially parallel orientation governs. As already discussed so far, there seems hopeless to invoke perpendicular orientation of lamellae or cylinders. Imposing the force fields perpendicular to a film is impossible, the electric fields are not applicable to thick film due to the electric breakdown, and the magnetic field needs very high field strength. A directional field caused by solvent evaporation may only provide a possibility. Nevertheless, it is impossible to overcome the thickness limitation of the perpendicular orientation of lamellae or cylinders induced by solvent evaporation, which is of an order of 1 μm, as discussed above. This is because of their strong tendency to align preferentially parallel to the substrate or free surface. Therefore, we should not insist in a direct way of the perpendicular orientation of cylinders or lamellae. Let us take a glance at controlling the orientation of the BCC lattice of spherical microdomains. Since there might be little preference in orientation of any particular crystallographic direction of the BCC lattice with respect to the surface of the sample film, it may be much easier to invoke perpendicular orientation of a key crystallographic direction of the BCC lattice by the solvent evaporation. If a ⟨111⟩ direction can be perpendicularly oriented, then coalescence of neighboring spheres on the ⟨111⟩ direction can be induced. As a consequence, perpendicular orientation of cylinders is spontaneously obtained. The point is that the initial structure is spherical and subsequent transformation from spheres to cylinders is induced by thermal annealing. Such a sophisticated tactics, however, can be rather simply conducted. If non-equilibrium spherical microdomains, which can be obtained when

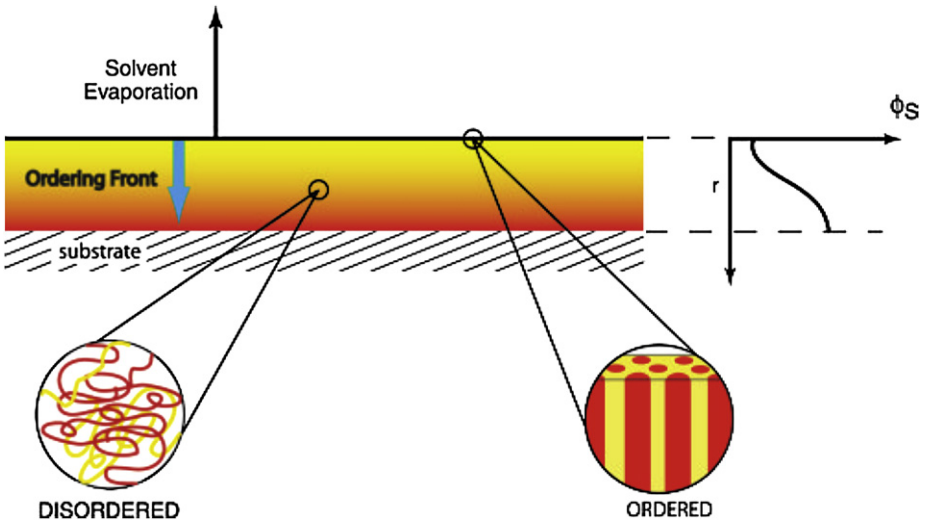

Fig. 9. Schematic representation of a surface-induced microphase separation and formation of an ordering front during the solution casting. As the solvent evaporates, concentration gradient (ϕ_S; volume fraction of the solvents) is induced such that the polymer concentration at the free surface of the solution is higher than that in the interior. As a consequence, microphase separation will take place at the surface of the solution, then it will grow down towards the interior. The directional solidification perpendicular to the film or solution surface proceeds with an ordering front parallel to the surface. Adopted from Ref. [97].

a cylinder-forming block copolymer is cast from a solution in selective solvent [98], are frozen in an as-cast film due to vitrification of one or both components of block species, the successive thermal annealing of the sample above their glass transition temperatures can induce coalescence of non-equilibrium spheres. Just the thermal annealing is very simple and convenient for the perpendicular orientation of cylinders. Moreover, this concept can be applied to any type of block species universally. In our recent study, we have conducted experiments according to this tactics with using a cylinder-forming SEBS triblock copolymer ($M_n = 6.6 \times 10^4$, $M_w/M_n = 1.03$, total volume fraction of PS is 0.16, forming PS cylinders) [99]. Fig. 11 schematically shows the tactics, which can be referred to as a directional coalescence of spheres. A selective solvent *n*-heptane was used for the solution casting, where *n*-heptane is good for PEB (polyethylenebutylene) and poor for PS. By the solution cast from the *n*-heptane solution, non-equilibrium PS spheres were formed in the as-cast film. And then the as-cast film was subjected to thermal annealing above T_g of PS, at 210 °C for this particular case, for 6 h. The thickness of the film was 0.7 mm.

Fig. 12 shows a 2D-SAXS pattern of the through view (a) and that of the edge view (b) for the annealed film. The geometrical relations between the film sample and an X-ray area detector for those views are schematically shown together. In the through view image, isotropic reflection rings are observed. On the contrary, many reflection peaks were observed in the edge view. The key point here is that many reflection spots (at relative q positions of 1, $\sqrt{3}$, $\sqrt{4}$, $\sqrt{7}$, and $\sqrt{9}$) being assigned to $\{10\bar{1}0\}$, $\{11\bar{2}0\}$, $\{20\bar{2}0\}$, $\{21\bar{3}0\}$, and $\{30\bar{3}0\}$ planes of the hexagonal lattice were just in line with the meridional direction. This is a clear evidence of the PS cylinders aligning perpendicularly to the film sample. The SAXS results were confirmed by transmission electron microscopy (TEM), as presented in Fig. 13. The PS microdomains are stained with RuO_4 so that they appear

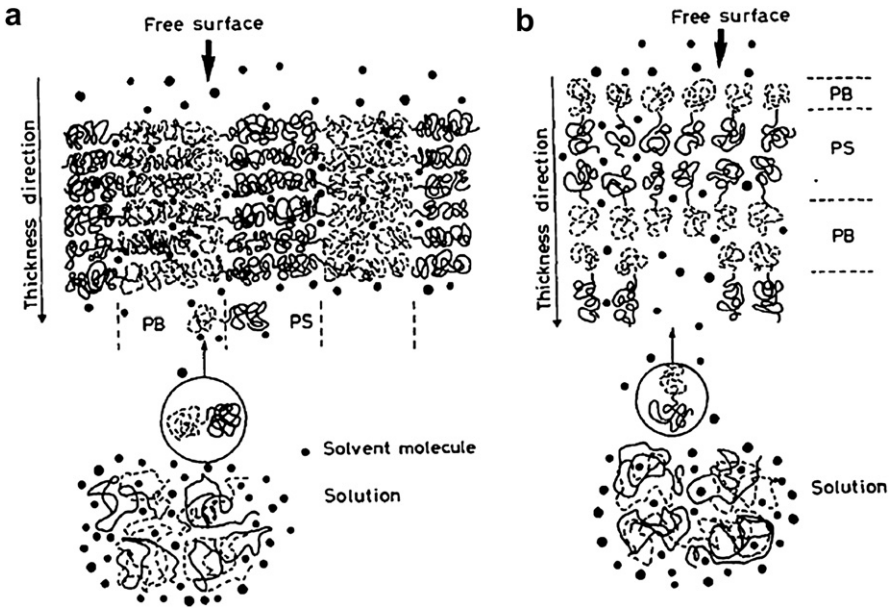

Fig. 10. Schematic illustrations providing a molecular picture of how the solvent molecule evaporates and comparing situations when the top surface of the polymer solution is covered with the ordering front of perpendicular lamellae (a) or parallel lamellae (b). This figure also explains how the ordering front proceeds; block copolymers still dissolved in the solution below the ordering front should be supplied from the solution phase to the ordering front. Adopted from Ref. [93].

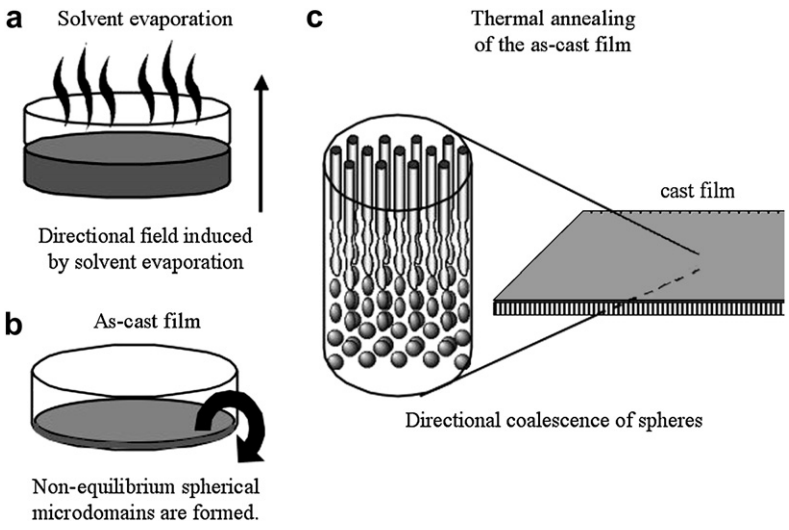

Fig. 11. Schematic illustrations showing tactics to invoke perpendicular orientation of cylinders in thick films by the directional coalescence of spheres through controlling the orientation of the BCC lattice of spherical microdomains in a directional field caused by solvent evaporation. If a ⟨111⟩ direction can be perpendicularly oriented by the directional field, then coalescence of neighboring spheres on the ⟨111⟩ direction gives rise to perpendicular orientation of cylinders. When a cylinder-forming block copolymer is cast from a solution in selective solvent, non-equilibrium spherical microdomains are frozen in an as-cast film due to vitrification of one or both components of block species. The successive thermal annealing of the sample above their glass transition temperatures can induce coalescence of non-equilibrium spheres. Adopted from Ref. [99].

dark in the TEM micrographs, while the PEB microdomains unstained appear bright. As shown in Fig. 13(a) and (b), perpendicular orientation of the PS cylinders is clearly confirmed. Furthermore, it can be also seen that the cylinders are arranged in the hexagonal lattice locally. Although not shown here, TEM of the edge view for the as-cast film revealed in some local regions a linear array of a limited number of PS spheres being approximately parallel to the film normal ***n***. The linear array of the PS spheres results in the

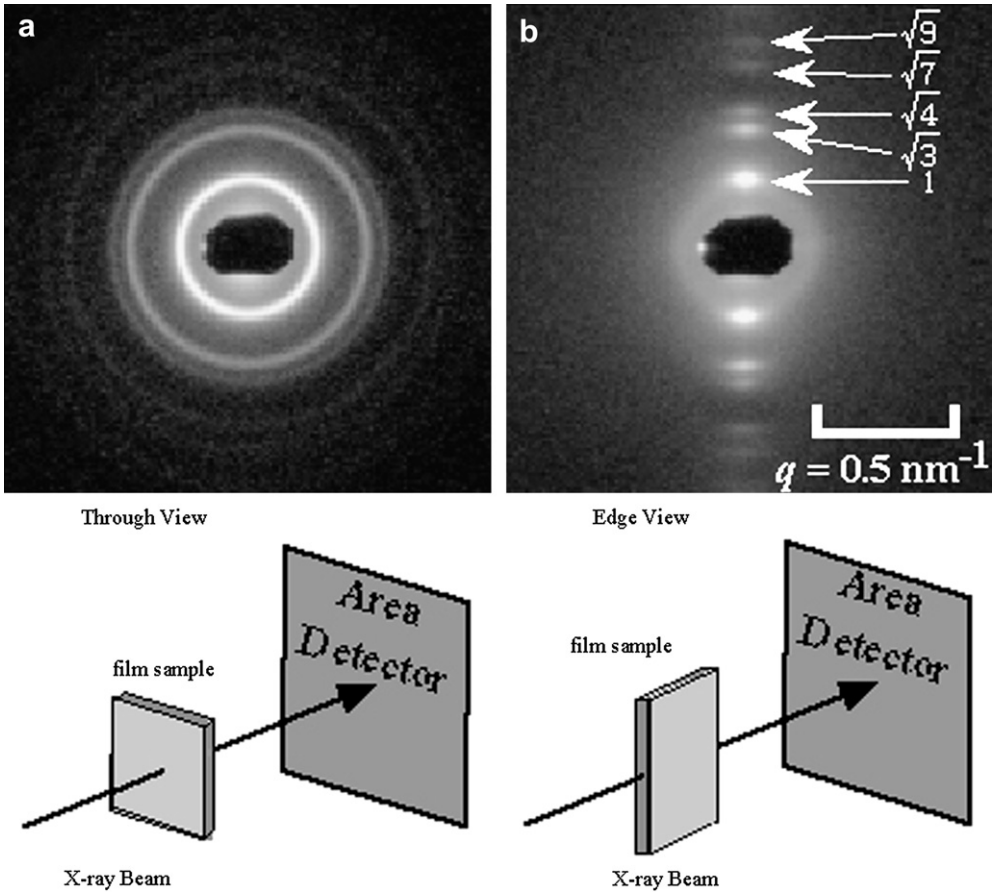

Fig. 12. 2D-SAXS pattern of the through view (a) and that of the edge view (b) for an annealed film of a cylinder-forming SEBS triblock copolymer ($M_n = 6.6 \times 10^4$, $M_w/M_n = 1.03$, total volume fraction of PS is 0.16, forming PS cylinders). The geometrical relations between the film sample and an X-ray area detector for those views are schematically shown together. The annealed film containing the perpendicular PS cylinders was prepared according to the tactics schematically shown in Fig. 11 (using *n*-heptane as selective solvent). By the solution cast from the *n*-heptane solution, non-equilibrium PS spheres were formed in the as-cast film. And then the as-cast film was subjected to thermal annealing above T_g of PS, at 210 °C for this particular case, for 6 h. The thickness of the film was 0.7 mm. Adopted from Ref. [99].

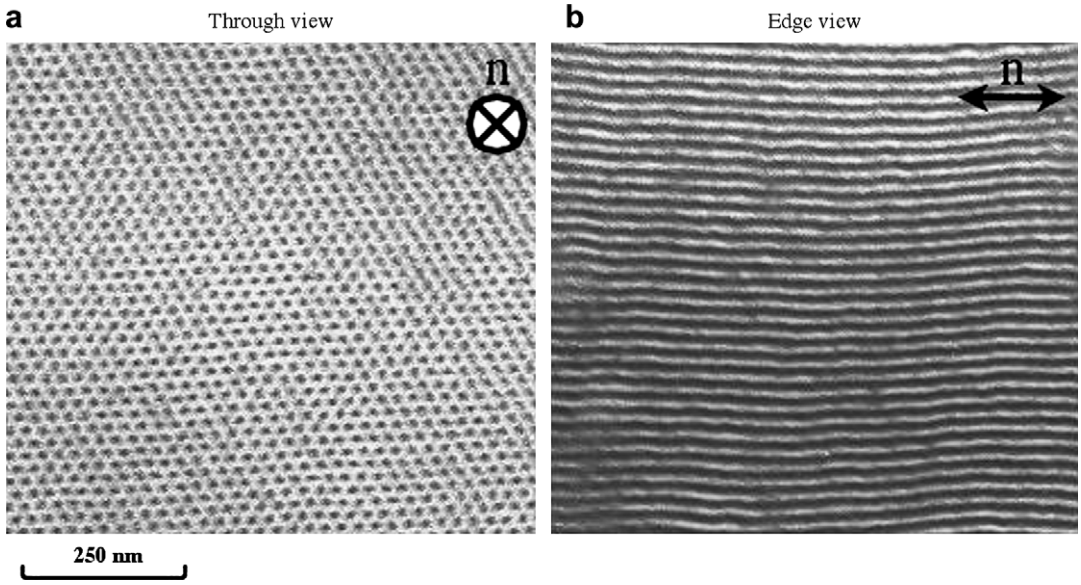

Fig. 13. Transmission electron micrographs of (a) through view and (b) edge view (***n***: film normal) for the SEBS annealed film containing the perpendicular PS cylinders. The PS microdomains are stained with RuO_4 so that they appear dark in the TEM micrographs, while the PEB microdomains unstained appear bright. Adopted from Ref. [99].

directional coalescence of the spheres (forming embryonic short cylinders), such that they can nucleate spontaneous orientation of thus-formed PS cylinders parallel to ***n*** (namely perpendicular to the film sample).

Since *n*-heptane is a good solvent for PEB while it is poor for PS, in the presence of the solvent the effective volume fraction of the PS phase is much decreased, which can alter the morphology. It is actually considered that the PS phase shrinks into spheres in an early stage of the solution cast process in the *n*-heptane solution. Upon the increase of the polymer concentration, the PS spheres are finally vitrified so that the SEBS sample cannot retrieve its equilibrium cylinder structures because of inhibition of coalescence of the glassy PS spheres. This scheme explains the fact that the PS spheres remained in the as-cast film after complete evaporation of the solvent (*n*-heptane), although the spheres are non-equilibrium. The thermal annealing above the glass transition temperature of the PS phase unlocks the frozen state so that the SEBS sample could attain the equilibrium microdomain structures (PS cylinders) [100].

Since the solvent dominantly exists in the PEB matrix phase during the solution cast, the solvent permeation paths in the PEB matrix should be parallel to ***n*** in order to attain the maximum solvent diffusivity. Whether the PS microdomains are spherical or cylindrical, the PS microdomains should not block the permeation paths. Such requirement forces a slip direction ⟨111⟩ of the BCC lattice to orient parallel to the permeation paths during the solvent evaporation. Note that the slip direction is the direction on which the nearest-neighbors are positioned and therefore those nearest-neighboring spheres coalesce each other along this direction. Since the slip direction in the as-cast film is so controlled to be normal to the film by the solvent evaporation according to the above-mentioned mechanism, the perpendicular orientation of thus-formed PS cylinders by the directional coalescence of the PS spheres is not stochastic but absolutely deterministic. Since the spherical microdomains do not necessarily favor orientation of the ⟨111⟩ direction being parallel to the substrate, the solvent evaporation (permeation) can easily align a ⟨111⟩ direction along with ***n*** even in the thick film. Those spheres are subjected to coalescence to each other along a ⟨111⟩ direction by thermal annealing, giving rise to perpendicular orientation of cylinders. At this moment, coalescence along with other ⟨111⟩ directions not giving rise to the perpendicular orientation should not take place. Embryonic short cylinders aligning parallel to ***n*** may dictate the right selection. Note that the embryonic short cylinders may be already formed during the solvent evaporation process by local coalescence of a limited number of spheres along with ***n***.

7. Future perspective

Imposing external fields, such as the force fields and the electric fields had been exclusively performed to control microdomain orientation. However, it has been more recognized that such special (or explicit) external fields are not necessarily required. As reported, for instance in Ref. [92], the simple addition of the homopolymer could be used to remarkably promote microdomain orientation without the use of external fields. This result clearly indicates that block copolymers self-organizing abilities still remaining unknown will be utilizable for performance of spontaneous orientation (or in other words self-orientation). In this article, we discussed even these kinds of the spontaneous orientation in the categories of implicit external fields, such as "surface fields" and "directional fields" because orientation of microdomains is always a consequence of responses of block copolymers brought into external fields, irrespective of whether the external fields are imposed explicitly (intentionally) or implicitly (unconsciously). Although some of these phenomena of the self-orientation have been already used in application-oriented researches towards nanotechnology, the mechanisms of self-orientation still remain ambiguous. Full understanding of the mechanisms is required and deserves a future work for innovative developments in the related nanotechnology. For instance, some of candidates are developments of a giant grain as big as possible, or perpendicularly-oriented cylinders in thick films (the thickness is of the order of, say, hundreds of microns) in which the cylinders with a diameter of tens of nanometers pierce straight from bottom to top surfaces. The aspect ratio of cylinders will become as large as $\sim 10^4$. In the meantime, other new phenomena of self-orientation and novel type of "directional fields" should be continuously explored for the sake of a breakthrough in the related nanotechnology, as well as great contributions to academia such as the materials science and the polymer science through understanding more about self-organization behaviors of chain molecules.

As for the explicit external fields, on the other hand, it is required to develop more effective methods, not only for a higher degree of orientation accomplished but also for a quicker response in larger size of samples. The roll casting method is an example of such a trial in the category of the force field. Trial of imposing a force field perpendicular to films or solutions may be a challenging subject. To put forward the limitation of the field strength due to the electric breakdown is an ultimate goal in the category of the electric field. Effectiveness of the magnetic field for amorphous block copolymers still remain unknown so that more thorough studies are requested. Meanwhile, technological advancement in manufacturing magnets for higher field strength is another important aspect.

References

[1] Hamley IW. Block copolymers. Oxford: Oxford Science Publications; 1999.
[2] Hamley IW. Introduction to block copolymers. In: Hamley Ian W, editor. Developments in block copolymer science and technology. London: John Wiley and Sons; 2004. p. 1 [chapter 1].
[3] Sakurai S, Okamoto S, Sakurai K. Melt behaviour of block copolymers. In: Hamley Ian W, editor. Developments in block copolymer science and technology. London: John Wiley and Sons; 2004. p. 127 [chapter 4].
[4] Mansky P, Harrison CK, Chaikin PM, Register RA, Yao N. Appl Phys Lett 1996; 93:2586.
[5] Park M, Harrison C, Chaikin PM, Register RA, Adamson H. Science 1997;276: 1401.
[6] De Rosa C, Park C, Thomas EL, Lotz B. Nature 2000;405:433.
[7] Park M, Chaikin PM, Register RA, Adamson DH. Appl Phys Lett 2001;79:257.
[8] Harrison C, Dagata JA, Adamson DH. Lithography with self-assembled block copolymer microdomains. In: Hamley Ian W, editor. Developments in block copolymer science and technology. London: John Wiley and Sons; 2004. p. 295 [chapter 9].
[9] Kitano H, Akasaka S, Inoue T, Chen F, Takenaka M, Hasegawa H, et al. Langmuir 2007;23:6404.
[10] Temple K, Kulbaba K, Power-Billard KN, Manners I, Leach KA, Xu T, et al. Adv Mater 2003;15:297.
[11] Honeker CC, Thomas EL. Chem Mater 1996;8:1702.
[12] Honeker CC, Thomas EL, Albalak RJ, Hajduk DA, Gruner SM, Capel MC. Macromolecules 2000;33:9395.
[13] Honeker CC, Thomas EL. Macromolecules 2000;33:9407.
[14] Chen ZR, Kornfield JA, Smith SD, Grothaus JT, Satkowski MM. Science 1997; 277:1248.
[15] Watanabe H. Rheology of multiphase polymeric systems. In: Araki T, Tran-Cong Q, Shibayama M, editors. Structure and properties of multi-phase polymeric materials. New York: Marcel Dekker; 1998. p. 317 [chapter 9].
[16] Mortensen K. J Phys Condens Matter 1996;8:A103.
[17] Hamley IW. Curr Opin Colloid Interface Sci 2000;5:342.
[18] Hamley IW, Castelletto V. Prog Polym Sci 2004;29:909.
[19] McConnell GA, Lin MY, Gast AP. Macromolecules 1995;28:6754.
[20] Gast AP. Curr Opin Colloid Interface Sci 1997;2:258.
[21] Pozzo DC, Walker LM. Macromolecules 2007;40:5801.
[22] Morrison FA, Mays JW, Muthukumar M, Nakatani AI, Han CC. Macromolecules 1993;26:5271.
[23] Angelescu DE, Waller JH, Adamson DH, Deshpande P, Chou SY, Register RA, et al. Adv Mater 2004;16:1736.
[24] Sakurai S, Kota T, Isobe D, Okamoto S, Sakurai K, Ono T, et al. J Macromol Sci Phys 2004;B43:1.
[25] Vigild ME, Eskimergen R, Mortensen K. Physica B 2004;350:E885.
[26] Winey KI, Patel SS, Larson RG, Watanabe H. Macromolecules 1993;26: 2542.
[27] Winey KI, Patel SS, Larson RG, Watanabe H. Macromolecules 1993;26: 4373.
[28] Okamoto S, Saijo K, Hashimoto T. Macromolecules 1994;27:5547.
[29] Pople JA, Hamley IW, Fairclough JPA, Ryan AJ, Hill G, Price C. Polymer 1999; 40:5709.
[30] Vigild ME, Chu C, Sugiyama M, Chaffin KA, Bates FS. Macromolecules 2001; 34:951.
[31] Harada T, Bates FS, Lodge TP. Macromolecules 2003;36:5440.
[32] Polis DL, Smith SD, Terrill NJ, Ryan AJ, Morse DC, Winey KI. Macromolecules 1999;32:4668.
[33] Qiao L, Winey KI, Morse DC. Macromolecules 2001;34:7858.
[34] Hermel TJ, Wu L, Hahn SF, Lodge TP, Bates FS. Macromolecules 2002;35:4685.
[35] Wu L, Lodge TP, Bates FS. J Rheol 2005;49:1231.
[36] Zhang Y, Wiesner U, Spiess HW. Macromolecules 1995;28:778.
[37] Gupta VK, Krishnamoorti R, Kornfield JA, Smith SD. Macromolecules 1995; 28:4464.
[38] Wang H, Newstein MC, Krishnan A, Balsara NP, Garetz BA, Hammouda B, et al. Macromolecules 1999;32:3695.
[39] Maring D, Wiesner U. Macromolecules 1997;30:660.
[40] Wang H, Kesani PK, Balsara NP, Hammouda B. Macromolecules 1997;30:982.
[41] Albalak RJ, Thomas EL. J Polym Sci Part B Polym Phys 1993;31:37.
[42] Albalak RJ, Thomas EL. J Polym Sci Part B Polym Phys 1994;32:341.
[43] Prasman E, Thomas EL. J Polym Sci Part B Polym Phys 1998;36:1625.
[44] Park C, Simmons S, Fetters LJ, Hsiao B, Yeh F, Thomas EL. Polymer 2000;41: 2971.
[45] Dair BJ, Avgeropoulos A, Hadjichristidis N, Capel M, Thomas EL. Polymer 2000;41:6231.
[46] Serpico JM, Wnek GE, Krause S, Smith TW, Luca DJ, Vanlaeken A. Macromolecules 1992;25:6373.
[47] Amundson K, Helfand E, Davis DD, Quan X, Patel SS, Smith SD. Macromolecules 1991;24:6546.
[48] Amundson K, Helfand E, Quan X, Smith SD. Macromolecules 1993;26:2698.
[49] Amundson K, Helfand E, Quan X, Hudson SD, Smith SD. Macromolecules 1994;27:6559.
[50] Morkved TL, Lu M, Urbas AM, Ehrichs EE, Jaeger HM, Mansky P, et al. Science 1996;273:931.
[51] Thurn-Albrecht T, Schotter J, Kästle GA, Emley N, Shibauchi T, Krusin-Elbaum L, et al. Science 2000;290:2126.
[52] Thurn-Albrecht T, De Rouchey J, Russell TP, Jaeger HM. Macromolecules 2000;33:3250.
[53] Thurn-Albrecht T, De Rouchey J, Russell TP, Kolb R. Macromolecules 2002;35: 8106.
[54] De Rouchey J, Thurn-Albrecht T, Russell TP, Kolb R. Macromolecules 2004;37: 2538.
[55] Gunkel I, Stepanow S, Thurn-Albrecht T, Trimper S. Macromolecules 2007; 40:2186.
[56] For instance, see <http://www.nims.go.jp/TML/>.
[57] Ferri D, Wolff D, Springer J, Francescangeli O, Laus M, Angeloni AS, et al. J Polym Sci Part B Polym Phys 1998;36:21.
[58] Hamley IW, Castelletto V, Lu ZB, Imrie CT, Itoh T, Al-Hussein M. Macromolecules 2004;37:4798.
[59] Osuji C, Ferreira PJ, Mao G, Ober CK, Sande JBV, Thomas EL. Macromolecules 2004;37:9903.
[60] Tomikawa N, Lu Z, Itoh T, Imrie CT, Adachi M, Tokita M, et al. Jpn J Appl Phys 2005;44:L711.
[61] Adachi M, Takazawa F, Tomikawa N, Tokita M, Watanabe J. Polym J 2007; 39:155.
[62] Ezure H, Kimura T, Ogawa S, Ito E. Macromolecules 1997;30:3600.
[63] Sata H, Kimura T, Ogawa S, Ito E. Polymer 1998;39:6325.
[64] Kawai T, Kimura T. Polymer 2000;41:155.
[65] Kimura T, Kawai T, Sakamoto Y. Polymer 2000;41:809.
[66] Grigorova T, Pispas S, Hadjichristidis N, Thurn-Albrecht T. Macromolecules 2005;38:7430.
[67] Yasui A, Kimura F, Kiyoshi T, Kimura T, Jeong Y, Sakurai S. Kobunshi Ronbunshu 2007;64:317 [in Japanese].
[68] Sakurai S, Yasui A, Kimura F, Kiyoshi T, Yamato M, Jeong Y, et al., in preparation.
[69] Knoll A, Horvat A, Lyakhova KS, Krausch G, Sevink GJA, Zvelindovsky AV, et al. Phys Rev Lett 2002;89:035501.
[70] Knoll A, Magerle R, Krausch G. J Chem Phys 2004;120:1105.
[71] Kimura T. Jpn J Appl Phys 2001;40:9318.
[72] Inaba H, Saitou T, Tozaki K, Hayashi H. J Appl Phys 2004;96:6127.
[73] Yamaguchi M, Tanimoto Y, editors. Magneto-science – magnetic field effects on materials: fundamentals and applications. Springer series in materials science, Band 89. Tokyo: Kodansha; 2006. p. 320.
[74] Sakurai S, Yasui A, Jeong Y, Kumada T, Koizumi S, Yamamoto K, et al., in preparation.
[75] Tanimoto Y, Fujiwara M, Sueda M, Inoue K, Akita M. Jpn J Appl Phys 2005;44: 9301.
[76] Kim SO, Solak HH, Stoykovich MP, Ferrier NJ, de Pablo JJ, Nealey PF. Nature 2003;424:411.
[77] Fasolka MJ, Harris DJ, Mayes AM, Yoonand M, Mochrie SGJ. Phys Rev Lett 1997;79:3018.
[78] Rockford L, Mochrie SGJ, Russell TP. Macromolecules 2001;34:1487.
[79] Karim A, Singh N, Sikka M, Bates FS, Dozier WD, Felcher GP. J Chem Phys 1994;100:1620.
[80] Peng J, Xuan Y, Wang H, Yang Y, Li B, Han Y. J Chem Phys 2004;120:11163.
[81] Cavicchi KA, Berthiaume KJ, Russell TP. Polymer 2005;46:11635.
[82] Zhang M, Yang L, Yurt S, Misner MJ, Chen JT, Coughlin EB, et al. Adv Mater 2007;19:1571.
[83] Kim S, Briber RM, Karim A, Jones RL, Kim HC. Macromolecules 2007;40:4102.
[84] Horvat A, Lyakhova KS, Sevink GJA, Zvelindovsky AV, Magerle R. J Chem Phys 2004;120:1117.
[85] van Dijk MA, van den Berg R. Macromolecules 1995;28:6773.
[86] Thomas EL, Kinning DJ, Alward DB, Henkee CS. Macromolecules 1987;20: 2934.
[87] Imaizumi K, Ono T, Kota T, Okamoto S, Sakurai S. J Appl Cryst 2003;36:976.
[88] Hashimoto T, Bodycomb J, Funaki Y, Kimishima K. Macromolecules 1999;32: 952.
[89] Bodycomb J, Funaki Y, Kimishima K, Hashimoto T. Macromolecules 1999;32: 2075.
[90] Hwang J, Huh J, Jung B, Hong JM, Park M, Park C. Polymer 2005;46:9133.
[91] Jeong U, Kim HC, Rodriguez RL, Tsai IY, Stafford CM, Kim JK, et al. Adv Mater 2002;14:274.
[92] Jeong U, Ryu DY, Kho DH, Kim JK, Goldbach JT, Kim DH, et al. Adv Mater 2004; 16:533.

[93] Turturro A, Gattiglia E, Vacca P, Viola GT. Polymer 1995;36:3987.
[94] Kim G, Libera M. Macromolecules 1998;31:2569.
[95] Ho RM, Tseng WH, Fan HW, Chiang YW, Lin CC, Ko BT, et al. Polymer 2005;46:9362.
[96] Lin Z, Kim DH, Wu X, Boosahda L, Stone D, Larose L, et al. Adv Mater 2002;14:1373.
[97] Kim SH, Misner MJ, Xu T, Kimura M, Russell TP. Adv Mater 2004;16:226.
[98] Sakurai S, Momii T, Taie K, Shibayama M, Nomura S, Hashimoto T. Macromolecules 1993;26:485.
[99] Sakurai S, Bando H, Yoshida H, Tsuji Y, Fukuoka R, Mouri M, et al. Perpendicular orientation of cylindrical microdomain in a block copolymer thick film. In: Sato T, editor. Chemistry, physics, and biology in macromolecular science. Osaka: Osaka University Press; 2007. p. 121.
[100] Umeda H, Aida S, Sakurai S, Kitagawa Y, Suda Y, Masamoto J, et al. Nihon Reoroji Gakkaishi 1997;25:217 [in Japanese].

Shinichi Sakurai is Associate Professor in Graduate School of Science and Technology, Kyoto Institute of Technology, Sakyo-ku, Kyoto 606-8585, Japan. He obtained his BS degree from Department of Polymer Chemistry, Faculty of Engineering, Kyoto University in 1984. He obtained his Dr. of Engineering degree from Division of Polymer Chemistry, Graduate School of Engineering, Kyoto University in 1992. Awards won by him are the following: (1) Prize for Excellence in Fiber Research, The Society of Fiber Science and Technology, Japan (2006) and (2) SAS2006 Award for Outstanding Service (2006). Presently, he is member of editorial advisory board, Polymer.